© 2017. Published by The Company of Biologists Ltd | Development (2017) 144, 1211-1220 doi:10.1242/dev.144071

Generation of thalamic neurons from mouse embryonic stem cells

Atsushi Shiraishi[1,2,3], Keiko Muguruma[1,3,‡] and Yoshiki Sasai[1,*]

ABSTRACT

The thalamus is a diencephalic structure that plays crucial roles in relaying and modulating sensory and motor information to the neocortex. The thalamus develops in the dorsal part of the neural tube at the level of the caudal forebrain. However, the molecular mechanisms that are essential for thalamic differentiation are still unknown. Here, we have succeeded in generating thalamic neurons from mouse embryonic stem cells (mESCs) by modifying the default method that induces the most-anterior neural type in self-organizing culture. A low concentration of the caudalizing factor insulin and a MAPK/ERK kinase inhibitor enhanced the expression of the caudal forebrain markers Otx2 and Pax6. BMP7 promoted an increase in thalamic precursors such as Tcf7l2$^+$/Gbx2$^+$ and Tcf7l2$^+$/Olig3$^+$ cells. mESC thalamic precursors began to express the glutamate transporter vGlut2 and the axon-specific marker VGF, similar to mature projection neurons. The mESC thalamic neurons extended their axons to cortical layers in both organotypic culture and subcortical transplantation. Thus, we have identified the minimum elements sufficient for *in vitro* generation of thalamic neurons. These findings expand our knowledge of thalamic development.

KEY WORDS: Mouse ES cells, Thalamus, Caudal forebrain, Self-organization, SFEBq

INTRODUCTION

The thalamus is a brain region in the diencephalon, which is located between the telencephalon and the midbrain. The thalamus receives and processes sensory signals from various subcortical systems including somatosensory, auditory, visual and motor systems. It sends the processed signals to the cerebral cortex via thalamocortical projections and receives regulatory feedback signals from the cortex via corticothalamic projections. The major function of the thalamus is to relay, gate and modulate sensory information to the cerebral cortex (Mitchell et al., 2014). During development, the thalamic primordium arises at a specific position of the neural tube. It is located anteroposteriorly in the caudal part of the forebrain and dorsoventrally in the alar plate or the dorsal part of the neural tube. Based on the concept that brain regions are specified by positional signals along the anteroposterior and dorsoventral axes of the neural tube (Stern, 2001), it seems likely that the thalamus could be specified by a set of patterning signals that are spatiotemporally expressed. However, the molecular mechanisms that mediate the development of the thalamic primordium remain largely unknown.

To reveal the molecular mechanisms and the minimum patterning signals necessary for thalamic development, we used an *in vitro* differentiation culture of embryonic stem cells (ESCs) (Muguruma and Sasai, 2012). This is a powerful tool for determining the minimum requirements for differentiation in a self-organizing tissue. We previously established an efficient culture system for selective neural differentiation of mouse and human ESCs, namely, serum-free culture of embryoid body-like aggregates with quick reaggregation (SFEBq) (Watanabe et al., 2005; Wataya et al., 2008). When cultured in a growth factor-free chemically defined medium (gfCDM), ESCs differentiate into hypothalamus, the anterior-most region of the neural tube, as a default fate. Insulin in the SFEBq culture functions as a weak caudalizing factor and induces structures of the midbrain-hindbrain boundary (MHB), including the isthmus (Wataya et al., 2008; Muguruma et al., 2010). The isthmus functions as an organizer that releases a key molecule, Fgf8, which further regulates the differentiation of the midbrain and the hindbrain (Wurst and Bally-Cuif, 2001). It is thought that insulin and Fgf8 are key molecules for the rostral-caudal specification of early neural development.

In the present study, we searched for an efficient method to differentiate mESCs into thalamic neurons by modifying the SFEBq culture. We found that a low concentration of insulin combined with MAPK/ERK kinase (MEK) inhibitor induced the expression of Pax6 and Otx2, markers for the caudal forebrain, while suppressing the midbrain marker En2. We further found that BMP7, which is expressed in thalamic primordium, promoted the induction of thalamic precursors such as Tcf7l2$^+$/Gbx2$^+$ and Tcf7l2$^+$/Olig3$^+$ cells. These mESC-derived thalamic precursors expressed the glutamate transporter vGlut2 (Slc17a6 – Mouse Genome Informatics). They selectively extended their neurites to explants of rat cerebral cortex in organotypic co-cultures. Furthermore, thalamic precursors transplanted in the subcortical regions of neonatal rat extended their axons through the white matter to the neocortex and innervated the upper layers. Thus, we have identified the minimum elements sufficient for *in vitro* generation of thalamic neurons. These findings expand our knowledge on the development of the thalamus and further open the way for regenerative medicine to address thalamic diseases.

RESULTS

Inhibition of the MEK pathway induces caudal forebrain in SFEBq culture

The rostral forebrain region is induced without any patterning signals in SFEBq culture. To induce caudal forebrain, we first attempted to caudalize the mESC-derived neural progenitors by adding insulin to the SFEBq culture (Fig. 1A,B). In qPCR analysis of regional marker genes (Fig. S1A-D), the titrated insulin (1 µg/ml; note that 7 µg/ml was used by Wataya et al., 2008; Muguruma et al., 2010) significantly decreased the expression of *Six3* and *Rax* (rostral forebrain) in day 7 mESC-differentiated cells (Fig. 1C,D). *Otx2*

[1]Laboratory for Organogenesis and Neurogenesis, RIKEN Center for Developmental Biology, Kobe 650-0047, Japan. [2] Laboratory of Growth Regulation, Institute for Virus Research, Graduate School of Medicine, Kyoto University, Kyoto 606-8507, Japan. [3]Laboratory for Cell Asymmetry, RIKEN Center for Developmental Biology, Kobe 650-0047, Japan.
*Deceased 5 August 2014

‡Author for correspondence (muguruma@cdb.riken.jp)

K.M., 0000-0002-3149-4408

Received 25 August 2016; Accepted 3 February 2017

Development (2017) 144, 1211-1220 doi:10.1242/dev.144071

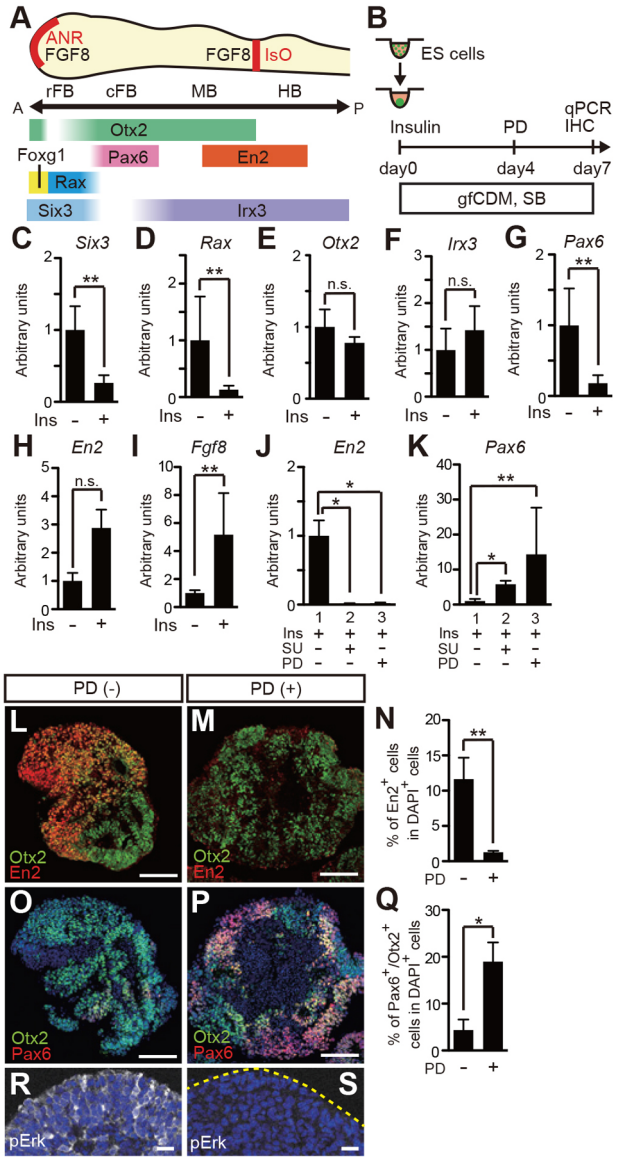

Fig. 1. Inhibition of the MEK pathway induces caudal forebrain in SFEBq culture. (A) Schematic showing the expression patterns of regional markers in the early embryonic neural tube (corresponding to E8). (B) Procedure for the differentiation of caudal forebrain cells from ESC culture. (C-I) qPCR analysis on day 7 for the expression of *Six3* (C), *Rax* (D), *Otx2* (E), *Irx3* (F), *Pax6* (G), *En2* (H) and *Fgf8* (I) (n=80 aggregates from five independent experiments). Insulin (1 µg/ml) was added to the culture on day 0. (J,K) qPCR analysis of SFEBq-cultured ESC aggregates on day 7 for the expression of *En2* (J) and *Pax6* (K) (n=40 aggregates from five independent experiments). FGF inhibitor (SU5402, 10 µM; SU) or MEK inhibitor (PD0325901, 1 µM; PD) were added to the culture on day 4. (L,M) Cryosections of aggregates on day 7, immunostained for Otx2 and En2. ESCs were cultured in insulin-containing medium (CDMI). MEK inhibitor was added to the culture on day 4. (N) Percentage of $En2^+$ cells in $DAPI^+$ cell aggregates on day 7 (n=96 aggregates from six independent experiments). (O,P) Sections adjacent to those shown in L and M, immunostained for Otx2 and Pax6. ESCs were cultured in CDMI. MEK inhibitor was added to the culture on day 4. (Q) Percentage of $Otx2^+/Pax6^+$ cells in $DAPI^+$ cell aggregates on day 7, immunostained for pErk. (n=96 aggregates from six independent experiments). (R,S) Cryosections of SFEBq-cultured ESC aggregates on day 7, immunostained for pErk. Yellow dashed line demarcates the outline of the aggregate. ANR, anterior neural ridge; cFB, caudal forebrain; HB, hindbrain; IsO, isthmic organizer; MB, midbrain; rFB, rostral forebrain; SB, SB431542. Scale bars: 100 µm (L,M,O,P); 20 µm (R,S). Nuclear counter staining (blue in O,P,R,S), DAPI. Each bar represents mean± s.d. *P<0.05; **P<0.01; n.s., not significant.

(caudal forebrain) and *Irx3* (caudal diencephalon and brain tissues caudal to it) were expressed without obvious changes in insulin-treated mESCs (Fig. 1E,F). *Pax6* (caudal forebrain) expression significantly decreased, whereas *En2* (around the isthmic organizer) expression substantially increased (Fig. 1G,H) in insulin-treated mESCs. Thus, titrated insulin certainly caudalized the rostral forebrain as expected; however, the induced region became midbrain rather than caudal forebrain. Actually, *Fgf8* expression was significantly increased by the insulin (Fig. 1I). These results raise the possibility that Fgf8 generates midbrain by acting as an inducing factor like the isthmic organizer and prevents the induction of caudal forebrain. To test this hypothesis, we tried to suppress the activity of FGF signaling.

FGF signaling is mediated by interaction with the FGF receptor (FGFR). It modulates downstream pathways including PI3K/AKT and MEK. To examine whether suppression of Fgf8 activity could induce the development of caudal forebrain, we applied downstream inhibitors of FGF signaling in SFEBq culture. Addition of FGFR inhibitor (SU5402, 10 nM) or MEK inhibitor (MEKi; PD0325901, 1 µM) on day 4 led to decreased expression of *En2* and *Fgf8* (Fig. 1J; Fig. S1E), whereas these genes were expressed without obvious changes after treatment with PI3K inhibitor (ZSTK474, 250 nM) (Fig. S1F,G, lane 3). In addition, treatment with PD0325901 (Fig. 1K, lane 3), compared with SU5402 (Fig. 1K, lane 2), significantly increased *Pax6* expression. Immunohistochemical analysis showed that $En2^+$ cells substantially decreased (Fig. 1L-N), whereas $Pax6^+/Otx2^+$ cells increased in PD0325901-treated mESCs on day 7 (Fig. 1O-Q). As expected, phosphorylation of ERK in the insulin-treated differentiating mESCs was markedly blocked by PD0325901 (Fig. 1R,S).

These findings suggest that suppression of Fgf8 activity via the MEK/ERK pathway induces the generation of $Pax6^+/Otx2^+$ caudal forebrain in SFEBq-cultured mESCs (Fig. S1H).

It is thought that the zona limitans intrathalamica (ZLI) is contributes to the development of caudal forebrain via secreted patterning signals, such as sonic hedgehog (Shh) and Wnts (Ishibashi and McMahon, 2002; Braun et al., 2003; Kiecker and Lumsden, 2004; Vue et al., 2009). We tested the effects of hedgehog agonist (SAG, 10 nM) or GSK3β inhibitor (CHIR99021, 1 µM) on the induction of caudal forebrain, but these compounds did not lead to any obvious changes in the expression of *En2*, *Fgf8* or *Pax6* on day 7 (Fig. S1I-K).

The treatment with MEKi and BMP7 induces thalamic primordium

Because the transcription factor Tcf7l2 starts to be expressed in the thalamus (embryonic day 9 onwards in mice) (Fig. 2A-F; Fig. S2A), we used *Tcf7l2::Venus* mESCs (Tcf7l2-Venus) to visualize thalamic precursors. However, Tcf7l2 is also expressed in regions other than the thalamus, including the midbrain and hindbrain (Fig. S2B,C). The transcription factors Gbx2 and Olig3, specific markers for thalamic primordium, are expressed in the marginal zone (MZ) and the ventricular zone (VZ) in thalamic primordium, respectively (Fig. 2A-F″). Thus, we used Tcf7l2 in combination with Gbx2 or Olig3 for identification of thalamic precursors.

As described above, PD0325901 induced generation of $Pax6^+/Otx2^+$ caudal forebrain; however, it only slightly increased $Tcf7l2\text{-}Venus^+$ cells on day 12 (Fig. S2D-K). We searched for further culture conditions to promote the generation of thalamic progenitors by modifying patterning signals in SFEBq culture. Wnt1, Wnt3a and BMP4 are expressed around the thalamic region (Furuta et al.,

Development (2017) 144, 1211-1220 doi:10.1242/dev.144071

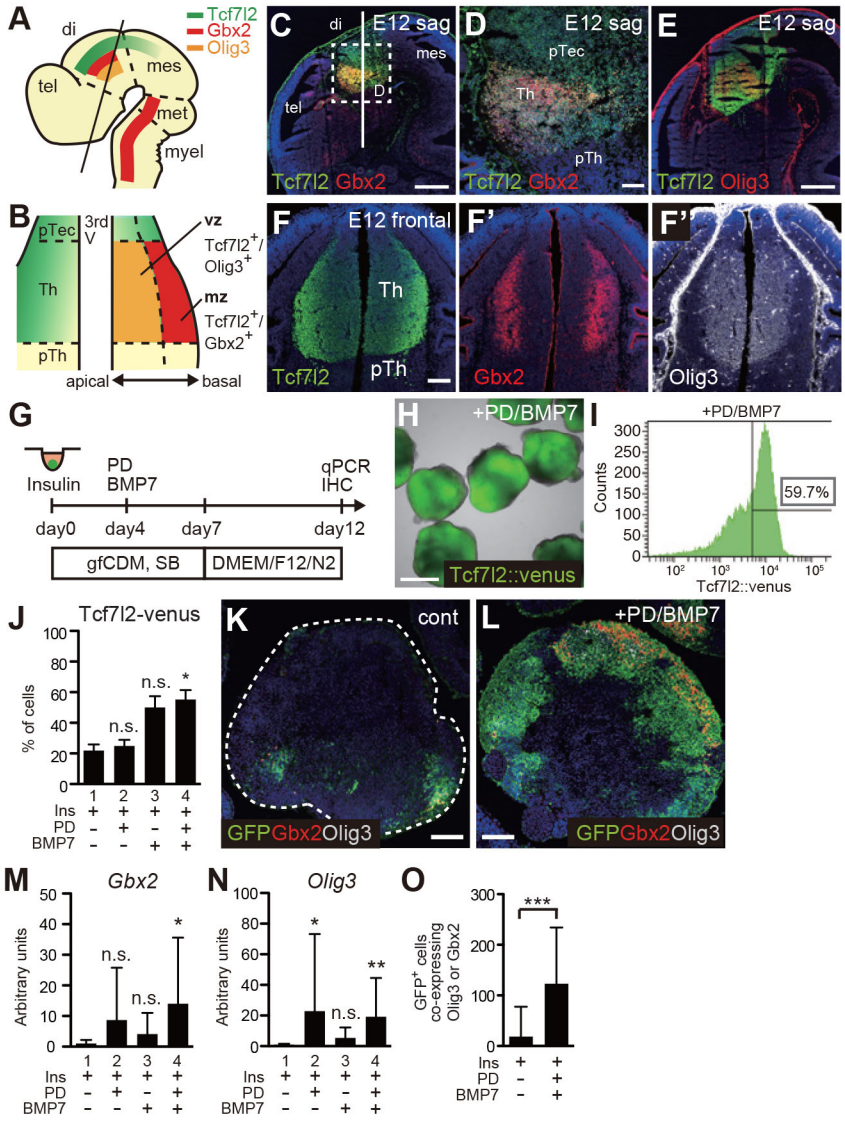

Fig. 2. Treatment with MEKi and BMP7 induces thalamic primordium. (A,B) Schematics showing the expression patterns of early thalamic markers from a lateral view (A) and in a frontal section (B). The solid line in A represents the plane of the frontal section in B. (C-F″) Expression of thalamic markers in E12 sagittal sections (C-E) and frontal sections (F-F″). Tcf7l2 is co-expressed with Gbx2 or Olig3 in thalamus, not in prethalamus and pretectum. Solid line in C represents the plane of the frontal sections shown in F-F″. Boxed area in C is shown at higher magnification in D. (G) Procedure for the differentiation of thalamic cells from mESC culture. MEK inhibitor (1 µM; PD) and/or BMP7 (30 ng/ml) were added to the culture on day 4. (H) SFEBq-cultured mESC aggregates (*Tcf7l2::Venus*) on day 12. (I,J) FACS analysis of mESC aggregates on day 12. A statistical difference was detected between insulin-treated mESCs and those treated with PD0325901 and BMP7 in addition to insulin. (K,L) Immunostaining of thalamic markers in mESC aggregates on day 12. Dashed line demarcates the outline of the aggregate. (M,N) qPCR analysis of SFEBq-cultured mESC aggregates on day 12 for the expression of *Gbx2* (M) and *Olig3* (N) (n=160 aggregates from ten independent experiments). Statistical differences are indicated. (O) The number of Tcf7l2-Venus$^+$ cells co-expressed with Gbx2 or Olig3. Treatment group, n=33 aggregates; control group, n=35. 3rd V, third ventricle; di, diencephalon; mes, mesencephalon; met, metencephalon; myel, myelencephalon; mz, mantle zone; pTec, pretectum; pTh, prethalamus; tel, telencephalon; Th, thalamus; vz, ventricular zone. Scale bars: 500 µm (C,E,H); 100 µm (D,F,K,L). Nuclear counter staining (blue in C-F,K,L), DAPI. Each bar represents mean±s.d. *P<0.05; **P<0.01; ***P<0.001; n.s., not significant.

1997; Suda et al., 2001; Braun et al., 2003; Ishibashi and McMahon, 2002). When these patterning molecules were added in SFEBq culture, qPCR analysis did not show any obvious changes in *Tcf7l2*, *Gbx2* and *Olig3* expression (Fig. S2L-N).

Bmp7 is expressed in the MZ of thalamic primordium (Suzuki-Hirano et al., 2011), and loss of *Bmp7* function causes caudal forebrain defects (Dudley and Robertson, 1997; Solloway and Robertson, 1999). When BMP7 (30 ng/ml) was added on day 4 with insulin and PD0325901 (IP) treatment in SFEBq culture (SFEBq/IP) (Fig. 2G), we observed Tcf7l2-Venus$^+$ mESC-derived cell aggregates in the culture on day 12 (Fig. 2H). The increase in Tcf7l2$^+$ cells was confirmed by fluorescence-activated cell sorting (FACS) analysis (Fig. 2I,J). Immunohistochemical analysis also showed that most of the cells in BMP7-treated mESC-aggregates were positive for Tcf7l2-Venus and co-expressed with Gbx2 or Olig3 (Fig. 2K,L). qPCR analysis showed that BMP7 in addition to IP treatment also significantly increased *Gbx2* and *Olig3* expression (Fig. 2M,N). The frequency of Venus$^+$ aggregates increased by treatment with PD0325901 plus BMP7. Within the Venus$^+$ aggregates, the number of Tcf7l2-Venus$^+$ co-expressing Olig3$^+$ or Gbx2$^+$ cells was significantly increased by the treatment (Fig. 2O).

BMP7 is well known as a dorsalizing factor in neural development, but we observed little change in expression of *Nkx6.1* (*Nkx6-1*), a specific marker for the ventral region (Fig. S2O). BMP7 also had little effect on the expression of regional marker genes along the anteroposterior axis (Fig. S2P-R).

Taken together, our findings indicate that BMP7 and PD0325901 cooperatively induce the differentiation of caudal forebrain, especially thalamus, in mESC-SFEBq culture (SFEBq/IPB, hereafter).

SFEBq/IPB-derived tissues composed subdomains of caudal forebrain

The caudal forebrain can be divided into several subdomains according to the expression of molecular markers (Fig. 3A; Fig. S3A-H). For example, Ascl1 and neurogenin 2 (Ngn2; Neurog2), which is expressed by precursors of glutamatergic projection neurons (Vue et al., 2007), show a complementary expression pattern (Fig. 3A-B″; Fig. S3A,A′). SFEBq/IPB cell aggregates formed a Tcf7l2-Venus$^+$ neuroepithelial-sphere structure with the apical side to the interior and labeled by strong N-cadherin (cadherin 2, Cdh2) and atypical protein kinase C (aPKC) expression (Fig. 3C,D). Ki67 (Mki67)$^+$ or phospho-histone H3$^+$ mitotic cells

Development (2017) 144, 1211-1220 doi:10.1242/dev.144071

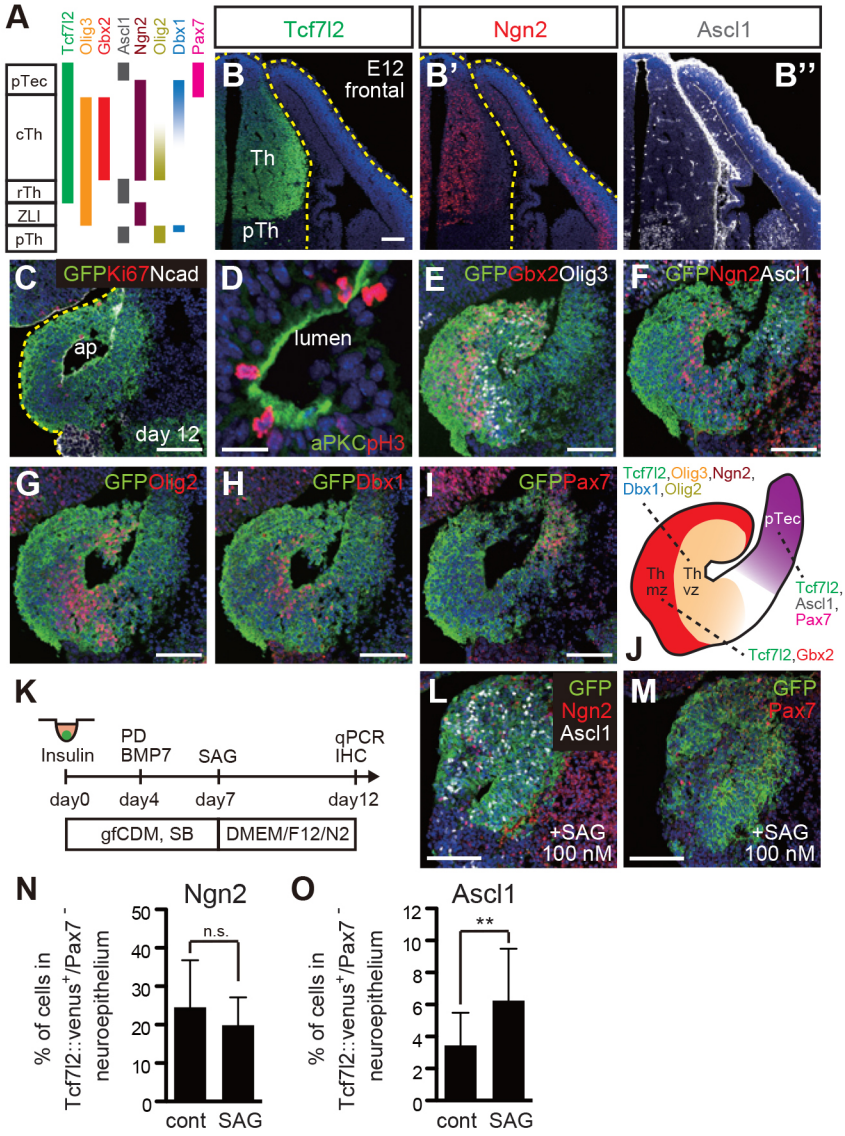

Fig. 3. SFEBq/IPB-derived tissues composed subdomains of caudal forebrain. (A) Schematic showing the expression patterns of progenitor markers in caudal forebrain. (B-B″) Expression of thalamic markers in an E12 mouse frontal section immunostained for Tcf7l2, Ngn2 and Ascl1. Yellow dashed line delineates the outline of the brain. (C-I) Cryosections of neural rosette in SFEBq-cultured mESC aggregates on day 12. mESCs were cultured in SFEBq/IPB. C, E and F are adjacent sections. (J) Schematic of the expression pattern of thalamic markers in the mESC aggregates. (K) Procedure for the differentiation of thalamic cells from mESC culture. SAG (100 nM) was added to the culture on day 7. (L,M) Adjacent cryosections of an aggregate treated with 100 nM SAG. (N,O) Percentage of cells expressing Ngn2 (N) or Ascl1 (O) in Tcf7l2-Venus^{+}/Pax7^{-} neuroepithelium in aggregates on day 12. Treatment group, n=19 neuroepithelium; control group, n=22. ap, apical surface; cTh, caudal thalamus; mz, mantle zone; pTec, pretectum; pTh, prethalamus; rTh, rostral thalamus; Th, thalamus; vz, ventricular zone; ZLI, zona limitans intrathalamica. Scale bars: 100 µm (B,C,E-I,L,M); 20 µm (D). Nuclear counter staining (blue in B,C,E-I,L,M), DAPI. Each bar represents mean±s.d. $^{**}P$<0.01; n.s., not significant.

were found at or near the apical area (Fig. 3C,D). The precursors of caudal thalamus that were identified by Tcf7l2-Venus^{+} and co-expression of Olig3, Ngn2, Olig2 or Dbx1 were localized in the inner zone close to the apical cavity, whereas those with Tcf7l2-Venus^{+}/Gbx2^{+} cells were located in the outer zone (Fig. 3E-H; Fig. S3B,F), recapitulating the stage of maturation along the apical-basal axis of the thalamic primordium. Cells expressing pretectal markers, Tcf7l2/Ascl1/Pax7, appeared in the region adjacent to the caudal thalamic primordium (Fig. 3A,F,I,J; Fig. S3B,D). A prethalamic marker, Isl1, or a basal plate marker, Nkx6.1, was expressed in the Tcf7l2-Venus^{-} regions (Fig. S3G,H). It is known by studies using mouse genetics that excess Shh signals enlarge the Ascl1-positive rostral thalamic subdomain (Vue et al., 2009). We tested the effect of excess Shh signals on the differentiation of mESC-derived cells. When SAG, a hedgehog agonist, was added in the cultures on day 7 (Fig. 3K), Tcf7l2-Venus^{+}/Ascl1^{+}/Pax7^{-} cells were greatly increased (Fig. 3L-O). This result indicates that rostral thalamic precursors were increased, consistent with the *in vivo* findings. Taken together, the results of the detailed analysis on marker expression patterns indicate that several subdomains of caudal forebrain, including thalamic primordium, differentiated in the SFEBq/IPB cell aggregates in a spatially distinct manner.

Regionalization of SFEBq/IPB-derived thalamic tissues

Tcf7l2 is expressed in the thalamus and the pretectum but not in the prethalamus in embryonic day (E)15 mice. Gbx2 and Sox2 are expressed in restricted regions, such that the thalamus is divided into a Gbx2^{+}/Tcf7l2^{+} caudo-medial portion and a Sox2^{+}/Tcf7l2^{+} rostral portion (Fig. 4A; Fig. S4A-F) (Nakagawa and O'Leary, 2001; Hashimoto-Torii et al., 2003). It is known that Sox2, a well-known marker for proliferative cells during embryogenesis, is also expressed by postmitotic cells in the thalamus (Vue et al., 2007). In SFEBq/IPB-derived thalamic tissue, Tcf7l2-Venus was intense in the basal region and mitotic Sox2^{+}/TuJ1 (Tubb3)$^{-}$ cells were found in the apical region, similar to the VZ (Fig. 4B,B′). Tcf7l2-Venus^{+}/Gbx2^{+} and Gbx2^{+}/Sox2^{+} cells were observed in SFEBq/IPB-derived thalamic tissue (Fig. 4C,C′). Sox2^{+} cells in the apical region expressed Ki67, a mitotic cell marker (Fig. 4D-D‴), whereas those in the basal region expressed TuJ1, a postmitotic neuronal marker (Fig. 4E-E‴). Immunohistochemical analysis showed that Gbx2^{+}, Sox2^{+}/TuJ1^{+} and Gbx2^{+}/Sox2^{+} cells were 7.3%, 23.1% and 2.8% of cells in Tcf7l2-Venus^{+} cells, respectively (Fig. 4F).

Collectively, we found that mESCs differentiated into thalamic primordium with a rostral-caudal spatial pattern in SFEBq/IPB culture. Furthermore, mESCs differentiated into a diencephalic

Development (2017) 144, 1211-1220 doi:10.1242/dev.144071

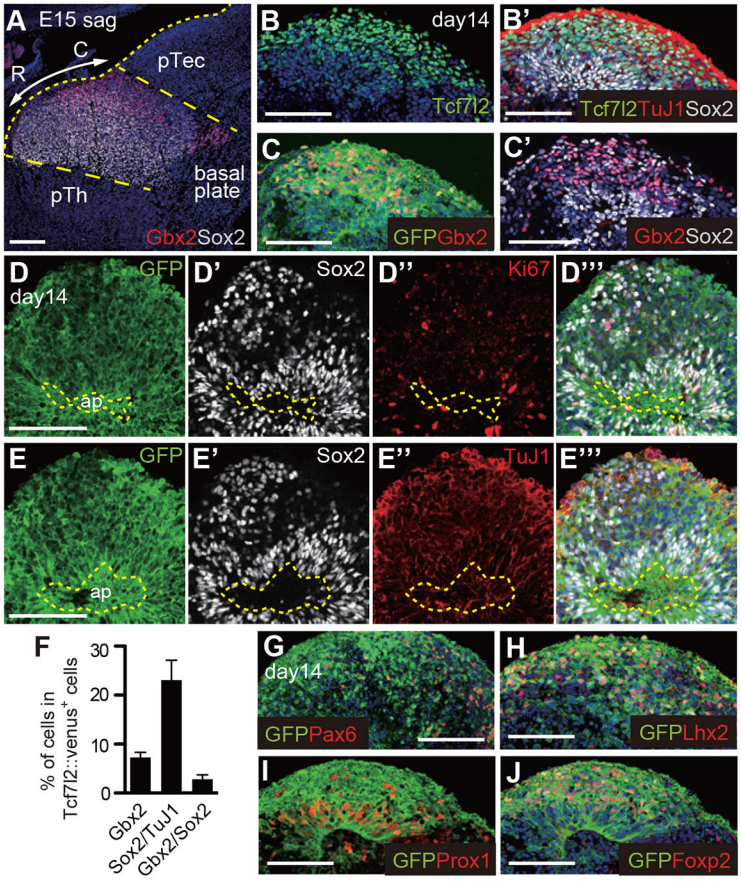

Fig. 4. Regionalization of SFEBq/IPB-derived thalamic tissues. (A) Expression of thalamic precursor markers in an E15 mouse sagittal section immunostained for Gbx2 and Sox2. C, caudal; R, rostral. Yellow dashed lines delineate the outline of the diencephalic regions. (B-C′) Adjacent sections of aggregates on day 14, immunostained for thalamic markers. (D-E‴) Postmitotic Tcf7l2$^+$/Sox2$^+$ precursors in aggregates on day 14. Yellow dashed line encircles the apical cavity. (F) Percentage of Gbx2$^+$, Sox2$^+$/TuJ1$^+$, or Gbx2$^+$/Sox2$^+$ cells in *Tcf7l2::Venus* cells on day 14 (n=72 aggregates from three independent experiments). (G-J) Expression of thalamic precursor markers in mESC aggregates on day 14. ap, apical side; pTec, pretectum; pTh, prethalamus. Scale bars: 200 µm (A); 100 µm (B-E,G-J). Each bar represents mean±s.d. Nuclear counter staining (blue), DAPI.

region including the thalamus, that is, Foxa2 (specific marker for the basal plate of embryonic brain) was expressed outside of the Tcf7l2-Venus$^+$ region (Fig. S4G,H). Foxa2$^+$ and Tcf7l2$^+$ cells were clearly divided in neuroepithelial structures in SFEBq/IPB culture. Pax6 was expressed in prethalamus and co-expressed with Tcf7l2 in a caudal part of pretectum (Suda et al., 2001), but not in the thalamus in E15 mice (Fig. S4I). Pax6 was expressed both in Tcf7l2-Venus$^-$ and Tcf7l2-Venus$^+$ regions in mESC-derived progenitors (Fig. 4G; Fig. S4J). Isl1, a marker for the prethalamus, was expressed in the part of Tcf7l2$^-$ regions that were distinct from those expressing basal plate markers, Nkx2.1 (Nkx2-1) or Nkx6.1 (Fig. S4K-M). These results suggest that mESCs differentiated into prethalamus, thalamus and pretectum with basal plate; in other words, our SFEBq/IPB culture can steer the differentiating region into diencephalon, including thalamus.

The transcription factors Lhx2 (Rétaux et al., 1999), Prox1 (Lavado and Oliver, 2007) and Foxp2 (Ferland et al., 2003) are co-expressed with Tcf7l2 in subsets of presumptive thalamic nuclei (Fig. S4N-P). These transcription factors were also expressed in Tcf7l2-Venus$^+$ cells cultured in SFEBq/IPB (Fig. 4H-J).

It is well known that hedgehog and/or Wnt/β-catenin signaling are involved in identification of thalamic progenitors (Ishibashi and McMahon, 2002; Braun et al., 2003; Bluske et al., 2012; Robertshaw et al., 2013; Kiecker and Lumsden, 2004; Vieira et al., 2005; Vue et al., 2009; Jeong et al., 2011). We tested the effects of a GSK3β inhibitor (CHIR99021, 1 µM) or a hedgehog agonist (SAG, 10 nM) on the SFEBq/IPB culture on day 7 (Fig. S4Q-T). The number of Tcf7l2-Venus$^+$ cells on day 14 in SFEBq/IPB culture did not change (Fig. S4U). However, addition of CHIR99021 caused an increase of Gbx2$^+$/Tcf7l2$^+$ cells (Fig. S4V, middle column), whereas the number of Sox2$^+$/TuJ1$^+$/Tcf7l2$^+$ cells did not change (Fig. S4W, middle column). Addition of SAG did not cause changes in the number of Gbx2$^+$/Tcf7l2$^+$ cells (Fig. S4V, right column) or Sox2$^+$/TuJ1$^+$/Tcf7l2$^+$ cells (Fig. S4W, right column). These results suggest that activation of Wnt signal by the GSK3β inhibitor CHIR99021 was involved in the induction of a caudal region of thalamus, but hedgehog signals had no substantial effect on regionalization of thalamus.

mESC-derived Tcf7l2$^+$ neurons extend their neurites like projection neurons

The thalamus contains vGlut2-expressing glutamatergic neurons that project their axons into the neocortex (Varoqui et al., 2002). The neuropeptide VGF is expressed in embryonic sensory thalamic nuclei and transported to the axon terminal (Fig. 5A-C; Fig. S5A,B′) (Sato et al., 2012). To examine the characteristics of SFEBq/IPB-cultured cells, we used 3D culture in collagen gel (Fig. 5D). The explants dissected from E15 mouse thalamus extended their axons radially in the collagen gel and the axons expressed VGF and vGlut2 (Fig. 5E-E″). The Tcf7l2-Venus$^+$ portion was dissected from SFEBq/IPB mESC-derived tissues on day 12 and cultured in collagen gel. Tcf7l2-Venus$^+$ neurites extended radially, similar to *in vivo* explants (Fig. S5C) and these neurites expressed VGF and vGlut2 (Fig. 5F-G‴, arrows; Fig. S5D-D‴′). We also observed VGF$^+$/vGlut2$^+$/Venus$^-$ neurites (Fig. 5F,F′, arrowheads), which were presumed to be neurites of the ventral posterior nucleus (Fig. S5A-B′). Most of the neurites emerging in the collagen gel cultures were Tcf7l2-Venus$^+$ (Fig. S5E-E‴). vGlut2$^+$ glutamatergic fibers were frequently observed, whereas GABAergic fibers were rarely observed (data not shown).

Development (2017) 144, 1211-1220 doi:10.1242/dev.144071

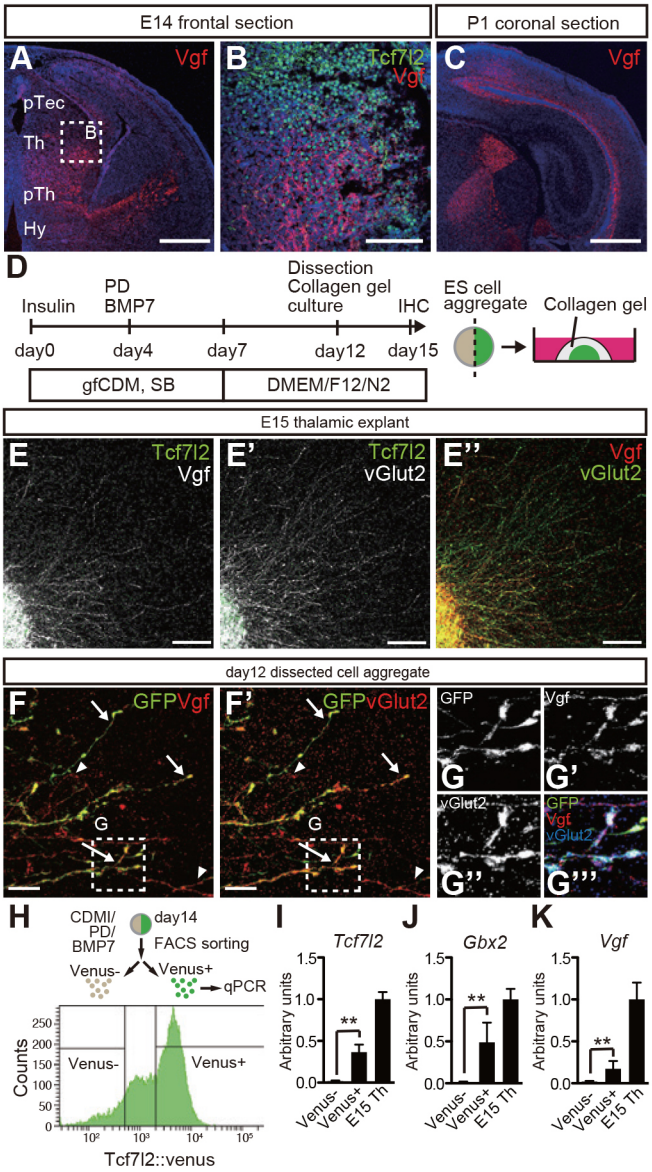

Fig. 5. mESC-derived Tcf7l2-Venus$^+$ neurites contain neuropeptides of thalamic projection neurons. (A-C) Expression of VGF nerve growth factor inducible (VGF) in an E14 mouse frontal section (A,B) and in a P1 coronal section (C). VGF proteins are localized in thalamocortical axons of sensory thalamic nuclei. Boxed area in A is shown at higher magnification in B. (D) Procedure for the collagen gel culture. (E-E″) Thalamic axons of explant dissected from E15 mouse at day 3 after collagen gel culture. (F,F′) mESC-derived thalamic neurites at day 3 after collagen gel culture. Arrows and arrowheads indicate VGF$^+$/vGlut2$^+$/GFP$^+$ and VGF$^+$/vGlut2$^+$/GFP$^-$ neurites, respectively. (G-G‴) High-magnification view of the boxed area in F. (H-K) SFEBq-cultured Tcf7l2-Venus$^+$ cells were sorted by FACS (N) and analyzed by qPCR on day 14 for the expression of *Tcf7l2* (I), *Gbx2* (J), and *Vgf* (K) (n=80 aggregates from five independent experiments). Total RNA from E15 thalamus was used as a control. **P<0.01. Hy, hypothalamus; pTec, pretectum; pTh, prethalamus; Th, thalamus. Scale bars: 500 µm (A,C); 100 µm (B,E); 20 µm (F). Each bar represents mean ±s.d. Nuclear counter staining (blue), DAPI.

Next, we sorted Tcf7l2-Venus$^+$ and Tcf7l2-Venus$^-$ cells on day 14 in SFEBq/IPB culture by FACS (Fig. 5H), and quantitative PCR analysis showed significantly greater *Tcf7l2* expression in the Venus$^+$ versus Venus$^-$ population (Fig. 5I). *Gbx2* and *Vgf* expression were also significantly higher in the Venus$^+$ fraction compared with the Venus$^-$ fraction (Fig. 5J,K). These data suggest that Tcf7l2-Venus$^+$ neurites show similar characteristics to thalamic cells *in vivo*.

mESC-derived axons project to neocortical tissues in organotypic culture and transplantation

To examine whether the SFEBq/IPB-cultured thalamic axons project to corresponding regions of neocortex, we performed organotypic culture in mESC-derived thalamic tissues with rat neonatal cortex (Fig. 6A). When rat thalamic explants (E15) were placed at the ventricular side of a rat cortical slice [postnatal day (P)1 to day 2] (Fig. 6B), thalamic fibers extended radially through the ventricular surface of the cortical slice as shown in previous reports (Yamamoto et al., 1989; Bolz et al., 1990; Molnár and Blakemore, 1991). When the dissected mESC-derived Tcf7l2-Venus$^+$ portion on day 15 was co-cultured with a neonatal (P2) rat cortical slice for 6 days, Venus$^+$ neurites extended into the cortical slice (Fig. 6C). Thalamocortical axons formed a branch in layer 4 of the cortex. RAR-related orphan receptor alpha (RORα) is expressed in layer 4 of the postnatal mouse cortex (Nakagawa and O'Leary, 2003). As shown in previous studies, Venus$^+$ neurites do not terminate in layer 4 labeled with RORα, but rather reach the marginal zone and then grow laterally along the pial surface. In our culture, immunostained Venus$^+$ neurons showed high intensity around the RORα$^+$ layer (Fig. 6C-F; Fig. S6A-C). RORα is known to be expressed in subsets of thalamic nuclei, and was actually expressed in the mESC-derived aggregates (Fig. S6C). Thus, RORα cells in the host cortical tissues could be migrated from the aggregates. However, this possibility was excluded by the observation that RORα$^+$ cell nuclei were not surrounded by GFP$^+$ perikarya (Fig. S6B). When we excluded data from the pial surface where axons grew laterally, the GFP intensity was correlated with that of RORα (correlation r=0.5776; Fig. 6G). To examine the preference of mESC-derived neurons for another target tissue, we also performed co-culture with a slice of cerebellum. In the cerebellar slice, Tcf7l2-Venus$^+$ neurites did not extend radially but showed a preference for fasciculate extension into the white matter as is the case with E15 thalamic explants co-cultured with a P2 rat cerebellar slice (Fig. S6D-H).

Finally, we performed the transplantation study to confirm the maturation and integration of mESC-derived thalamic neurons in P5 rat brain. To label the transplanted neurons with extended axon, we generated *ROSA26::MT/MG* knocked-in Tcf7l2-Venus mESCs. The dissociated mESC-derived thalamic precursors on day 15 were injected into caudate putamen (Fig. 6H; 20,000 cells per neonate). The grafted cells were observed in subcortical regions such as caudate putamen, white matter and cortical plate. They had characteristic properties observed in thalamus *in vivo* (e.g. cruciate dendrites) (Fig. 6I-L; Fig. S6I-J″) (Friedlander et al., 1981). This morphology could resemble that of oligodendrocytes, but these cells were not labeled with an oligodendrocyte marker, oligodendrocyte specific protein (OSP) (Fig. S6K-M″). The membrane Tomato$^+$ transplanted cells extended their axons through the white matter towards the neocortex into the upper cortical layers (Fig. 6M,N). Such axonal projection patterns are similar to those of thalamic neurons transplanted into the postnatal rat (Kurotani et al., 1993). These findings show that we established an *in vitro* differentiation method for thalamus.

DISCUSSION

In vitro generation of thalamic neurons from mESCs

Based on accumulated knowledge of differentiation of other brain regions (Wataya et al., 2008; Muguruma et al., 2010), we

Development (2017) 144, 1211-1220 doi:10.1242/dev.144071

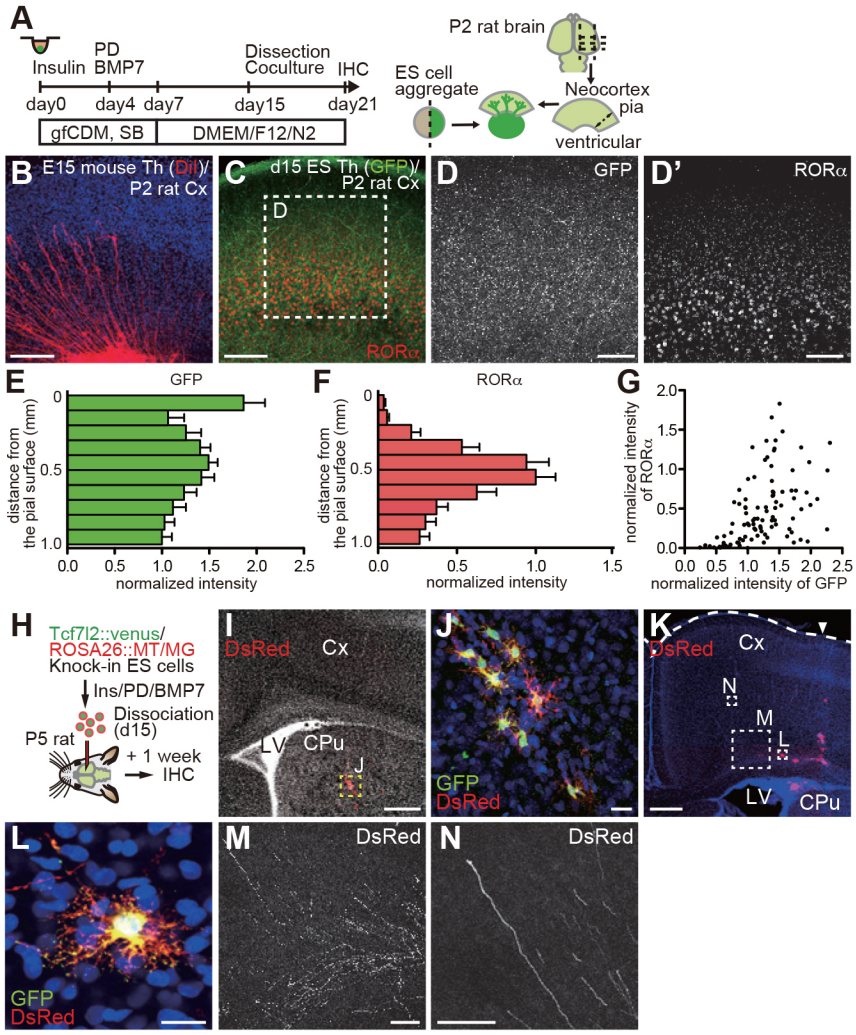

Fig. 6. mESC-derived thalamic neurons extend neurites into neocortex. (A) Procedure for ESC culture and co-culture with rat cortical slices. (B) Co-culture of E15 mouse thalamic explant and P2 rat cortical slice on day 6. DiI was injected in thalamic explant. (C) Co-culture of ESC aggregate and rat cortical slice on day 6 of co-culture. Tcf7l2-Venus$^+$ neurites showed radial extension into the cortical slice. Tcf7l2-Venus$^+$ neurites did not terminate in layer 4 (labeled with RORα) but reached the marginal zone, but these neurites were denser in RORα$^+$ layer of the cortex. (D,D′) High-magnification view of the boxed area in C. (E,F) Distribution histograms of normalized intensity of GFP (E) and RORα (F) constructed with 0.1 mm bins (n=11 slices). Note that obtained values 0-0.1 mm from the pia are large because of ectopic lateral extension on the pial surface. (G) Graph comparing normalized intensity of GFP with that of RORα (n=99 bins, exclusive of values 0-0.1 mm from the pia of each slice). r=0.5776, P<0.0001, Spearman's correlation coefficient by rank. (H) Schematic of the method for transplantation. (I) Grafted neurons in the caudate putamen at 1 week after transplantation. (J) High-magnification view of the boxed area in I. (K) Neurites from grafted neurons at 1 week after transplantation. (L) High-magnification view of the boxed area in K. A neuron in the white matter was integratable and was a Tcf7l2$^+$ thalamic-like neuron. (M) High-magnification view of the boxed area in K. Membrane Tomato$^+$ neurites of grafted neurons turned up from the white matter into the cortical plate. (N) High-magnification view of the boxed area in K. Membrane Tomato$^+$ neurites reached in upper layer of the cortex. CPu, caudate putamen; Cx, cortex; LV, lateral ventricle; Th, thalamus. Scale bars: 200 µm (B,C); 100 µm (D,M,N); 500 µm (I,K); 20 µm (J,L). Nuclear counter staining (blue in B,J-L, gray in I), DAPI.

successfully generated thalamic tissues in mESC culture using a 3D self-organizing system. In our SFEBq/IPB-cultured ESC aggregates, thalamic tissues co-existed with thalamus-neighboring tissues including basal plate, prethalamus and pretectum (Figs 3 and 4). This phenomenon may be consistent with the hypothesis that formation of ZLI from basal plate and regionalization of caudal forebrain should result from interaction between transcription factors expressed in prethalamus and thalamus (Suda et al., 2001; Braun et al., 2003; Hirata et al., 2006; Scholpp et al., 2007).

The spatial pattern of induced thalamic neurons in the neural rosettes resembled the following *in vivo* spatial expression pattern: Tcf7l2-Venus$^+$/Olig3$^+$ VZ cells were localized in the inner zone close to the apical cavity, and Tcf7l2-Venus$^+$/Gbx2$^+$ MZ cells were away from the apical side (Fig. 3E). Once caudal forebrain was induced in the cell aggregates on day 7, thalamic tissues self-organized without exogenous patterning signals (Fig. 4). Treatment with GSK3β inhibitor showed no obvious changes but tended to increase the Tcf7l2-Venus$^+$/Gbx2$^+$ population. Somatosensory or visual nuclei emerge from the rostral part of the thalamus, whereas auditory and some cognitive nuclei emerge from the caudal part of the thalamus. The mechanism of thalamic nuclear organization, however, remains largely elusive. Our mESC-derived 3D-cultured thalamus could be a new tool for addressing this question.

In this study, we offer new insight into patterning signals for early thalamic development. The efficient induction of thalamic tissues was triggered by transient treatment with the MEK inhibitor PD0325901 and BMP7. FGFR inhibitor or MEK inhibitor induced caudal forebrain tissues in mESC aggregates by suppressing midbrain induction (Fig. 1), which is consistent with a previous study of *Fgfr1* mutant mice (Lahti et al., 2012). These data suggest that robustness of the caudal forebrain and MHB regions depends on the FGF signaling pathway. *Fgfr1* is weakly expressed throughout neural tube and *Fgfr2* and *Fgfr3* are expressed in caudal forebrain (Ishibashi and McMahon, 2002; Walshe and Mason, 2000). Actually, when a piece of isthmic tissue or FGF8-soaked beads are implanted in the caudal forebrain of chick embryos, they induce ectopic midbrain-hindbrain regions (Crossley et al., 1996; Martinez et al., 1999). Therefore, the MEK/ERK pathway is thought to remain inactive because the caudal forebrain is somewhat distant from the FGF8 signaling center (isthmic organizer).

Compared with FGF, Wnt and Shh, BMP signals have been rarely discussed in terms of thalamic early development. In the process of establishing this thalamic differentiation method, we found that the addition of BMP7 along with MEK inhibitor promoted the induction of thalamic primordium (Fig. 2). However, the mechanism for thalamic induction by BMP signals remains unclear. The findings obtained from an *in vitro* system can inform future *in vivo* analysis in order to increase our understanding of early thalamic development.

Development (2017) 144, 1211-1220 doi:10.1242/dev.144071

Remaining questions and future applications

The mESC-derived neurons contained neuropeptides, such as VGF, similar to those of thalamic projection neurons (Fig. 5) and projected their axons into the cortex (Fig. 6). The thalamus relays sensory inputs to the neocortex and modulates cognitive processes including memory, attention and decision-making (Mitchell et al., 2014). Recently, several studies have supported a correlation between neurodevelopmental/psychiatric disorders and defects in the thalamocortical neural network (Parnaudeau et al., 2013; Chun et al., 2014; Wells et al., 2016). Thalamocortical axons also have been shown to influence the survival and identity of postmitotic cortical neurons via thalamus-derived molecules including VGF (Sato et al., 2012; Li et al., 2013; Gerstmann and Zimmer, 2015). Understanding the pathogenesis of neurodevelopmental disorders, however, remains challenging. In a preliminary study, we are applying the differentiation culture to human induced pluripotent stem cells. In the future, analysis of thalamic development using our ESC-derived thalamus might be useful for elucidating the mechanisms underlying human neurodevelopmental disorders.

MATERIALS AND METHODS

ESC culture

mESCs (EB5, *Tcf7l2::Venus*, and *ROSA26::MT/MG* knocked-in *Tcf7l2::Venus*) were maintained as described (Watanabe et al., 2005). For SFEBq culture, mESCs were dissociated into single cells in 0.25% trypsin-EDTA and quickly re-aggregated in differentiation medium (3000 cells per 150 µl well) in 96-well low-cell-adhesion plates (Thermo Fisher Scientific, 174925). The differentiation medium used during days 0-7 was gfCDM (Johansson and Wiles, 1995; Wataya et al., 2008), consisting of Iscove's modified Dulbecco's medium/Ham's F-12 1:1, chemically defined lipid concentrate, penicillin/streptomycin, monothioglycerol (450 µM), apo-transferrin (15 µg/ml) and crystallization-purified bovine serum albumin (5 mg/ml, Sigma). The medium was supplemented with insulin (1 µg/ml) and SB431542 (10 µM, Tocris) on day 0 (the starting day of differentiation culture).

Generation of knock-in ESC lines

To generate the targeting construct, we used the rapid two-recombination (EG construction) method (Ikeya et al., 2005). Briefly, the 5′ arm (6.2 kbp) and 3′ arm (4.2 kbp) were excised *in vitro* from the BAC clones (129J mouse) using the Red/ET cloning. The cDNA of *Venus*, encoding a yellow variant of GFP (Nagai et al., 2002), was fused in-frame into the first exon of the *Tcf7l2* gene at the initial ATG. A *Pgk* promoter-driven neomycin-resistance selection cassette flanked by *loxP* sites was inserted downstream of *Venus*. After electroporation of the linearized vector into EB5 ESCs, homologous recombinant ESCs were selected with neomycin and then screened. Three targeted clones (#1-2, #1-11, #2-34) were confirmed by Southern blot analysis with the 3′, 5′ and *neo* probes. The floxed *PGK-neo* cassette was removed from #1-11 by transient transfection with Cre-expressing plasmid using Amaxa Nucleofector. The resultant subclones (clone #1-11-10, #1-11-11 and #1-11-18) were confirmed by genotyping PCR with the *Tcf7l2* and *neo* probes, and they exhibited indistinguishable abilities to differentiate into Tcf7l2^{+} thalamic progenitors; subclone #1-11-18 was mainly used for the experiments shown in this report. The *ROSA26::MT/MG* knocked-in *Tcf7l2::Venus* mESC line was produced in a similar fashion. The resultant subclones (clone #1-11-11-1 and #1-11-11-2) were confirmed by Tomato signal and genotyping PCR with the *ROSA* probes, and exhibited indistinguishable abilities to differentiate into Tcf7l2^{+} thalamic progenitors; subclone #1-11-11-2 was used for the experiments shown in this report.

Neural differentiation culture

For the neural differentiation culture, PD0325901 (1 µM, Stemgent) and BMP7 (30 ng/ml, R&D Systems) were added to gfCDM containing insulin on day 4. On day 7, the cell aggregates were transferred to a Petri dish in DMEM/F12 GlutaMAXI/N2/10% fetal bovine serum.

Immunohistochemistry

Immunohistochemistry (IHC) was performed as described (Watanabe et al., 2005). Images were analyzed with vHCS Discovery Toolbox software (Thermo Fisher Scientific) and ImageJ (National Institutes of Health; http://rsb.info.nih.gov/ij/rsb.info.nih.gov/ij/). Values shown in graphs represent mean±s.d. Antibodies to the following proteins were used at the indicated dilutions: Pax6 (1:250, PRB278P, BAbCO; 1:200, sc-7750, Santa Cruz Biotechnology), Otx2 (1:100, ab21990, abcam; 1:100, sc-30659, Santa Cruz Biotechnology), En2 (1:100, sc-8111, Santa Cruz Biotechnology), Foxg1 (1:5000, AS3514, custom, Watanabe et al., 2005), Rax (1:3000, MS8407-3, custom, Ikeda et al., 2005), Six3 (1:1000, AS3984, custom, Wataya et al., 2008), Irx3 (1:1000, M230, Takara), phospho-Erk1/2 (1:1000, 4370, Cell Signaling), Tcf7l2 (1:1000, 2569, Cell Signaling; 1:1000, 05-511, Millipore), Gbx2 (1:10,000, no.1-1, custom, Muguruma et al., 2015; 1:500, AF4638, R&D Systems), Olig3 (1:500, MAB2456, R&D Systems), GFP (1:1000, 04404-84, Nacalai Tesque; 1:1000, 598, MBL), neurogenin 2 (shown as Ngn2; 1:1000, sc-19233, Santa Cruz Biotechnology), Mash1 (shown as Ascl1; 1:200, 556604, BD Pharmingen), Ki67 (1:1000, NCL-Ki67p, Novocastra; 1:200, 556003, BD Pharmingen), N-cadherin (1:1000, 610920, BD Transduction), PKCζ (shown as aPKC; 1:100, sc-216, Santa Cruz Biotechnology), phospho-histone H3 (1:500, 9706, Cell Signaling), Olig2 (1:1000, AB9610, Millipore), Dbx1 (1:2000, Ms-1513, custom synthetic peptide antigen conjugated to KLH; antibodies to C+DEDEEGEEDEEITVS were raised in guinea pig and antiserum was affinity purified), Pax7 (1:100, MAB1675, R&D Systems), TuJ1 (1:300, MMS-435P, Covance), Sox2 (1:250, sc-17320, Santa Cruz Biotechnology), Lhx2 (1:100, sc-19344, Santa Cruz Biotechnology), Prox1 (1:200, MAB5654, Millipore), Foxp2 (1:1000, ab16046, abcam), VGF (1:5000, ab69989, abcam), vGlut2 (1:1000, AB5907, Chemicon), RORα (1:100, sc-6062, Santa Cruz Biotechnology), DsRed (1:500, 632496, Clontech), Isl1 (1:100, 40.3A4, Developmental Studies Hybridoma Bank), Nkx6.1 (1:200, HPA036774, Sigma), Foxa2 (1:400, 8186S, Cell Signaling; 1:300, AF2400, R&D Systems), TTF-1 (shown as Nkx2.1; 1:100, 12373S, Cell Signaling), oligodendrocyte specific protein (shown as OSP; 1:500, ab53041, abcam), MAP2 (1:500, M9942, Sigma). Fluorescence-tagged secondary antibodies were as follows: Cy2-, Cy3-, Cy5-, Alexa Fluor 488- or Alexa Fluor 647-conjugated (Jackson Immuno Research). The signal for En2 was detected using biotinylated anti-goat IgG with Cy2- or Cy3-conjugated streptavidin (Vector Laboratories). DAPI was used for counterstaining the nuclei (Molecular Probes). Stained sections were analyzed with LSM710 and LSM780 confocal microscopes (Carl Zeiss). Images were assembled using Adobe Photoshop CS5.

Quantitative PCR

Quantitative PCR was performed using the 7500 Fast Real Time PCR System (Applied Biosystems) and data were normalized to *Gapdh* expression. PCR primers are listed in Table S1. The values shown on graphs represent mean±s.d. For quantitative analysis, 8-16 aggregates were examined for each experiment, which was repeated at least three times.

FACS

For FACS analysis, cells were counted with FACSAria (Becton Dickinson), and the data were analyzed with the FACSDiva software (Becton Dickinson). The cells were dispersed to single cells using Nerve-Cell Culture System/Dissociation Solutions (Sumitomo Bakelite) and analyzed at 4°C. The cells were dispersed on day 12 or day 14, and filtered through a Cell Strainer (BD Biosciences).

Collagen gel culture

The procedure for collagen gel culture was modified as described previously (Shirasaki et al., 1995). ESC aggregates were dissected and embedded in collagen gel matrix. ESC aggregates were cultured in DMEM/F12/GlutaMAXI/N2 medium at 37°C in 5% CO_2 for 3 days.

Organotypic co-culture

Organotypic co-culture was carried out using the modified procedure in Yamamoto et al. (1992). Briefly, fetal mice (E15) were removed from

pregnant females (ICR), and the whole brain was dissected from each fetal mouse and kept in cold DMEM medium. Thalamic explants were dissected in the medium under a binocular microscope. A Tcf7l2-Venus^{+} portion of mESC aggregate (day 15) was dissected in medium for neural differentiation culture. The cortical coronal slices and cerebellar sagittal slices (300-500 µm thickness) were dissected from newborn rats (P1-2). These neural tissues were kept in cold DMEM medium.

Rat slices (cortex or cerebellum), and thalamic explant or dissected cell aggregates were plated on the collagen-coated membrane (Coster, Transwell-COL #3942), separated at a distance of less than 0.5 mm. Thalamic explant or dissected cell aggregate was plated so that it faced the ventral side of the cortical or cerebellar slice. Serum-free, hormone-supplemented medium (DMEM/F12/GlutaMAXI/N2) was used to enhance neuronal survival and to suppress glial proliferation. In addition, the culture medium contained 5% fetal bovine serum for the first 2 days.

For the distribution histogram of normalized intensity of GFP and RORα, ten regions of interest (0.1 mm×0.4 mm) per slice were manipulated from pia to 1 mm depth. Images were analyzed with ImageJ.

Transplantation

The transplanted cells were *Tcf7l2::Venus*/*ROSA26::MT/MG* mESCs dispersed by Nerve-Cell Culture System/Dissociation Solutions on day 15. To perform the transplantation, P5 neonatal rats were deeply anesthetized by inhalation of sodium pentobarbital. Two microliters of cell suspension (20,000 cells per µl) was injected into the white matter of right hemisphere of each neonate using a 26-gauge needle attached to a 10-µl Hamilton syringe (Hamilton). The brain was dissected 1 week after transplantation, sectioned at a 50-µm thickness, and the sections were immunostained.

Animals

ICR mice and SD rats were obtained from Nihon-SLC. The animals were cared for in accordance with the Regulations on Animal Experiments of RIKEN.

Statistical analyses

All data are shown as mean±s.d. Statistical analyses were performed with PRISM software (GraphPad, version 6). Statistical significance was tested by unpaired Mann–Whitney test (nonparametric) for two-group comparisons or Kruskal–Wallis with Dunn's test for multiple-group comparisons.

Acknowledgements

We thank F. Matsuzaki, M. Eiraku and M. Ohgushi for discussion; M. Kawada for technical advice for generation of knocked-in mESCs; and M. Shiraishi, C. Shiraishi, K. Shiraishi, K. Fujiwara, M. Takeichi, T. Hirano, and all members of the Sasai group and Matsuzaki group for support and encouragement. A.S. offers special thanks to Yoshiki Sasai for enthusiastic mentoring, and sincere respect for his integrity to science and precious time he spent on the Sasai group.

Competing interests

The authors declare no competing or financial interests.

Author contributions

K.M. conceived and supervised this project. A.S performed the main body of experiments and data analysis. K.M. and A.S. wrote the manuscript. Y.S. designed this project. K.M. acquired funding. All authors read and approved the final manuscript.

Funding

This work was supported by the Program for Intractable Disease Research utilizing Disease-specific iPS cells from the Japan Science and Technology Agency and the Japan Agency for Medical Research and Development (AMED) [16bm0609002h0105 to K.M.].

Supplementary information

Supplementary information available online at http://dev.biologists.org/lookup/doi/10.1242/dev.144071.supplemental

References

Bluske, K. K., Vue, T. Y., Kawakami, Y., Taketo, M. M., Yoshikawa, K., Johnson, J. E. and Nakagawa, Y. (2012). β-Catenin signaling specifies progenitor cell identity in parallel with Shh signaling in the developing mammalian thalamus. *Development* **139**, 2692-2702.

Bolz, J., Novak, N., Götz, M. and Bonhoeffer, T. (1990). Formation of target-specific neuronal projections in organotypic slice cultures from rat visual cortex. *Nature* **346**, 359-362.

Braun, M. M., Etheridge, A., Bernard, A., Robertson, C. P. and Roelink, H. (2003). Wnt signaling is required at distinct stages of development for the induction of the posterior forebrain. *Development* **130**, 5579-5587.

Chun, S., Westmoreland, J. J., Bayazitov, I. T., Eddins, D., Pani, A. K., Smeyne, R. J., Yu, J., Blundon, J. A. and Zakharenko, S. S. (2014). Specific disruption of thalamic inputs to the auditory cortex in schizophrenia models. *Science* **344**, 1178-1182.

Crossley, P. H., Martinez, S. and Martin, G. R. (1996). Midbrain development induced by FGF8 in the chick embryo. *Nature* **380**, 66-68.

Dudley, A. T. and Robertson, E. J. (1997). Overlapping expression domains of bone morphogenetic protein family members potentially account for limited tissue defects in BMP7 deficient embryos. *Dev. Dyn.* **208**, 349-362.

Ferland, R. J., Cherry, T. J., Preware, P. O., Morrisey, E. E. and Walsh, C. A. (2003). Characterization of Foxp2 and Foxp1 mRNA and protein in the developing and mature brain. *J. Comp. Neurol.* **460**, 266-279.

Friedlander, M. J., Lin, C. S., Stanford, L. R. and Sherman, S. M. (1981). Morphology of functionally identified neurons in lateral geniculate nucleus of the cat. *J. Neurophysiol.* **46**, 80-129.

Furuta, Y., Piston, D. W. and Hogan, B. L. (1997). Bone morphogenetic proteins (BMPs) as regulators of dorsal forebrain development. *Development* **124**, 2203-2212.

Gerstmann, K. and Zimmer, G. (2015). Fine-tuning of cortical progenitor proliferation by thalamic afferents. *Neural Regen. Res.* **10**, 887-888.

Hashimoto-Torii, K., Motoyama, J., Hui, C.-C., Kuroiwa, A., Nakafuku, M. and Shimamura, K. (2003). Differential activities of Sonic hedgehog mediated by Gli transcription factors define distinct neuronal subtypes in the dorsal thalamus. *Mech. Dev.* **120**, 1097-1111.

Hirata, T., Nakazawa, M., Muraoka, O., Nakayama, R., Suda, Y. and Hibi, M. (2006). Zinc-finger genes Fez and Fez-like function in the establishment of diencephalon subdivisions. *Development* **133**, 3993-4004.

Ikeda, H., Osakada, F., Watanabe, K., Mizuseki, K., Haraguchi, T., Miyoshi, H., Kamiya, D., Honda, Y., Sasai, N., Yoshimura, N. et al. (2005). Generation of Rx+/Pax6+ neural retinal precursors from embryonic stem cells. *Proc. Natl. Acad. Sci. USA* **102**, 11331-11336.

Ikeya, M., Kawada, M., Nakazawa, Y., Sakuragi, M., Sasai, N., Ueno, M., Kiyonari, H., Nakao, K. and Sasai, Y. (2005). Gene disruption/knock-in analysis of mONT3: vector construction by employing both in vivo and in vitro recombinations. *Int. J. Dev. Biol.* **49**, 807-823.

Ishibashi, M. and McMahon, A. P. (2002). A sonic hedgehog-dependent signaling relay regulates growth of diencephalic and mesencephalic primordia in the early mouse embryo. *Development* **129**, 4807-4819.

Jeong, Y., Dolson, D. K., Waclaw, R. R., Matise, M. P., Sussel, L., Campbell, K., Kaestner, K. H. and Epstein, D. J. (2011). Spatial and temporal requirements for sonic hedgehog in the regulation of thalamic interneuron identity. *Development* **138**, 531-541.

Johansson, B. M. and Wiles, M. V. (1995). Evidence for involvement of activin A and bone morphogenetic protein 4 in mammalian mesoderm and hematopoietic development. *Mol. Cell. Biol.* **15**, 141-151.

Kiecker, C. and Lumsden, A. (2004). Hedgehog signaling from the ZLI regulates diencephalic regional identity. *Nat. Neurosci.* **7**, 1242-1249.

Kurotani, T., Yamamoto, N. and Toyama, K. (1993). Development of neural connections between visual cortex and transplanted lateral geniculate nucleus in rats. *Dev. Brain Res.* **71**, 151-168.

Lahti, L., Peltopuro, P., Piepponen, T. P. and Partanen, J. (2012). Cell-autonomous FGF signaling regulates anteroposterior patterning and neuronal differentiation in the mesodiencephalic dopaminergic progenitor domain. *Development* **139**, 894-905.

Lavado, A. and Oliver, G. (2007). Prox1 expression patterns in the developing and adult murine brain. *Dev. Dyn.* **236**, 518-524.

Li, H., Fertuzinhos, S., Mohns, E., Hnasko, T. S., Verhage, M., Edwards, R., Sestan, N. and Crair, M. C. (2013). Laminar and columnar development of barrel cortex relies on thalamocortical neurotransmission. *Neuron* **79**, 970-986.

Martinez, S., Crossley, P. H., Cobos, I., Rubenstein, J. L. and Martin, G. R. (1999). FGF8 induces formation of an ectopic isthmic organizer and isthmocerebellar development via a repressive effect on Otx2 expression. *Development* **126**, 1189-1200.

Mitchell, A. S., Sherman, S. M., Sommer, M. A., Mair, R. G., Vertes, R. P. and Chudasama, Y. (2014). Advances in understanding mechanisms of thalamic relays in cognition and behavior. *J. Neurosci.* **34**, 15340-15346.

Molnár, Z. and Blakemore, C. (1991). Lack of regional specificity for connections formed between thalamus and cortex in coculture. *Nature* **351**, 475-477.

Muguruma, K. and Sasai, Y. (2012). In vitro recapitulation of neural development using embryonic stem cells: from neurogenesis to histogenesis. *Dev. Growth Differ.* **54**, 349-357.

Muguruma, K., Nishiyama, A., Ono, Y., Miyawaki, H., Mizuhara, E., Hori, S., Kakizuka, A., Obata, K., Yanagawa, Y., Hirano, T. et al. (2010). Ontogeny-recapitulating generation and tissue integration of ES cell-derived Purkinje cells. *Nat. Neurosci.* **13**, 1171-1180.

Muguruma, K., Nishiyama, A., Kawakami, H., Hashimoto, K. and Sasai, Y. (2015). Self-organization of polarized cerebellar tissue in 3D culture of human pluripotent stem cells. *Cell Rep.* **10**, 537-550.

Nagai, T., Ibata, K., Park, E. S., Kubota, M., Mikoshiba, K. and Miyawaki, A. (2002). A variant of yellow fluorescent protein with fast and efficient maturation for cell-biological applications. *Nat. Biotech.* **20**, 87-90.

Nakagawa, Y. and O'Leary, D. D. (2001). Combinatorial expression patterns of LIM-homeodomain and other regulatory genes parcellate developing thalamus. *J. Neurosci.* **21**, 2711-2725.

Nakagawa, Y. and O'Leary, D. D. M. (2003). Dynamic patterned expression of orphan nuclear receptor genes RORalpha and RORbeta in developing mouse forebrain. *Dev. Neurosci.* **25**, 234-244.

Parnaudeau, S., O'Neill, P.-K., Bolkan, S. S., Ward, R. D., Abbas, A. I., Roth, B. L., Balsam, P. D., Gordon, J. A. and Kellendonk, C. (2013). Inhibition of mediodorsal thalamus disrupts thalamofrontal connectivity and cognition. *Neuron* **77**, 1151-1162.

Rétaux, S., Rogard, M., Bach, I., Failli, V. and Besson, M. J. (1999). Lhx9: a novel LIM-homeodomain gene expressed in the developing forebrain. *J. Neurosci.* **19**, 783-793.

Robertshaw, E., Matsumoto, K., Lumsden, A. and Kiecker, C. (2013). Irx3 and Pax6 establish differential competence for Shh-mediated induction of GABAergic and glutamatergic neurons of the thalamus. *Proc. Natl. Acad. Sci. USA* **110**, E3919-E3926.

Sato, H., Fukutani, Y., Yamamoto, Y., Tatara, E., Takemoto, M., Shimamura, K. and Yamamoto, N. (2012). Thalamus-derived molecules promote survival and dendritic growth of developing cortical neurons. *J. Neurosci.* **32**, 15388-15402.

Scholpp, S., Foucher, I., Staudt, N., Peukert, D., Lumsden, A. and Houart, C. (2007). Otx1l, Otx2 and Irx1b establish and position the ZLI in the diencephalon. *Development* **134**, 3167-3176.

Shirasaki, R., Tamada, A., Katsumata, R. and Murakami, F. (1995). Guidance of cerebellofugal axons in the rat embryo: directed growth toward the floor plate and subsequent elongation along the longitudinal axis. *Neuron* **14**, 961-972.

Solloway, M. J. and Robertson, E. J. (1999). Early embryonic lethality in Bmp5; Bmp7 double mutant mice suggests functional redundancy within the 60A subgroup. *Development* **126**, 1753-1768.

Stern, C. D. (2001). Initial patterning of the central nervous system: how many organizers? *Nat. Rev. Neurosci.* **2**, 92-98.

Suda, Y., Hossain, Z. M., Kobayashi, C., Hatano, O., Yoshida, M., Matsuo, I. and Aizawa, S. (2001). Emx2 directs the development of diencephalon in cooperation with Otx2. *Development* **128**, 2433-2450.

Suzuki-Hirano, A., Ogawa, M., Kataoka, A., Yoshida, A. C., Itoh, D., Ueno, M., Blackshaw, S. and Shimogori, T. (2011). Dynamic spatiotemporal gene expression in embryonic mouse thalamus. *J. Comp. Neurol.* **519**, 528-543.

Varoqui, H., Schäfer, M. K., Zhu, H., Weihe, E. and Erickson, J. D. (2002). Identification of the differentiation-associated Na+/PI transporter as a novel vesicular glutamate transporter expressed in a distinct set of glutamatergic synapses. *J. Neurosci.* **22**, 142-155.

Vieira, C., Garda, A.-L., Shimamura, K. and Martinez, S. (2005). Thalamic development induced by Shh in the chick embryo. *Dev. Biol.* **284**, 351-363.

Vue, T. Y., Aaker, J., Taniguchi, A., Kazemzadeh, C., Skidmore, J. M., Martin, D. M., Martin, J. F., Treier, M. and Nakagawa, Y. (2007). Characterization of progenitor domains in the developing mouse thalamus. *J. Comp. Neurol.* **505**, 73-91.

Vue, T. Y., Bluske, K., Alishahi, A., Yang, L. L., Koyano-Nakagawa, N., Novitch, B. and Nakagawa, Y. (2009). Sonic hedgehog signaling controls thalamic progenitor identity and nuclei specification in mice. *J. Neurosci.* **29**, 4484-4497.

Walshe, J. and Mason, I. (2000). Expression of FGFR1, FGFR2 and FGFR3 during early neural development in the chick embryo. *Mech. Dev.* **90**, 103-110.

Watanabe, K., Kamiya, D., Nishiyama, A., Katayama, T., Nozaki, S., Kawasaki, H., Watanabe, Y., Mizuseki, K. and Sasai, Y. (2005). Directed differentiation of telencephalic precursors from embryonic stem cells. *Nat. Neurosci.* **8**, 288-296.

Wataya, T., Ando, S., Muguruma, K., Ikeda, H., Watanabe, K., Eiraku, M., Kawada, M., Takahashi, J., Hashimoto, N. and Sasai, Y. (2008). Minimization of exogenous signals in ES cell culture induces rostral hypothalamic differentiation. *Proc. Natl. Acad. Sci. USA* **105**, 11796-11801.

Wells, M. F., Wimmer, R. D., Schmitt, L. I., Feng, G. and Halassa, M. M. (2016). Thalamic reticular impairment underlies attention deficit in Ptchd1$^{Y/-}$ mice. *Nature* **532**, 58-63.

Wurst, W. and Bally-Cuif, L. (2001). Neural plate patterning: upstream and downstream of the isthmic organizer. *Nat. Rev. Neurosci.* **2**, 99-108.

Yamamoto, N., Kurotani, T. and Toyama, K. (1989). Neural connections between the lateral geniculate nucleus and visual cortex in vitro. *Science* **245**, 192-194.

Yamamoto, N., Yamada, K., Kurotani, T. and Toyama, K. (1992). Laminar specificity of extrinsic cortical connections studied in coculture preparations. *Neuron* **9**, 217-228.

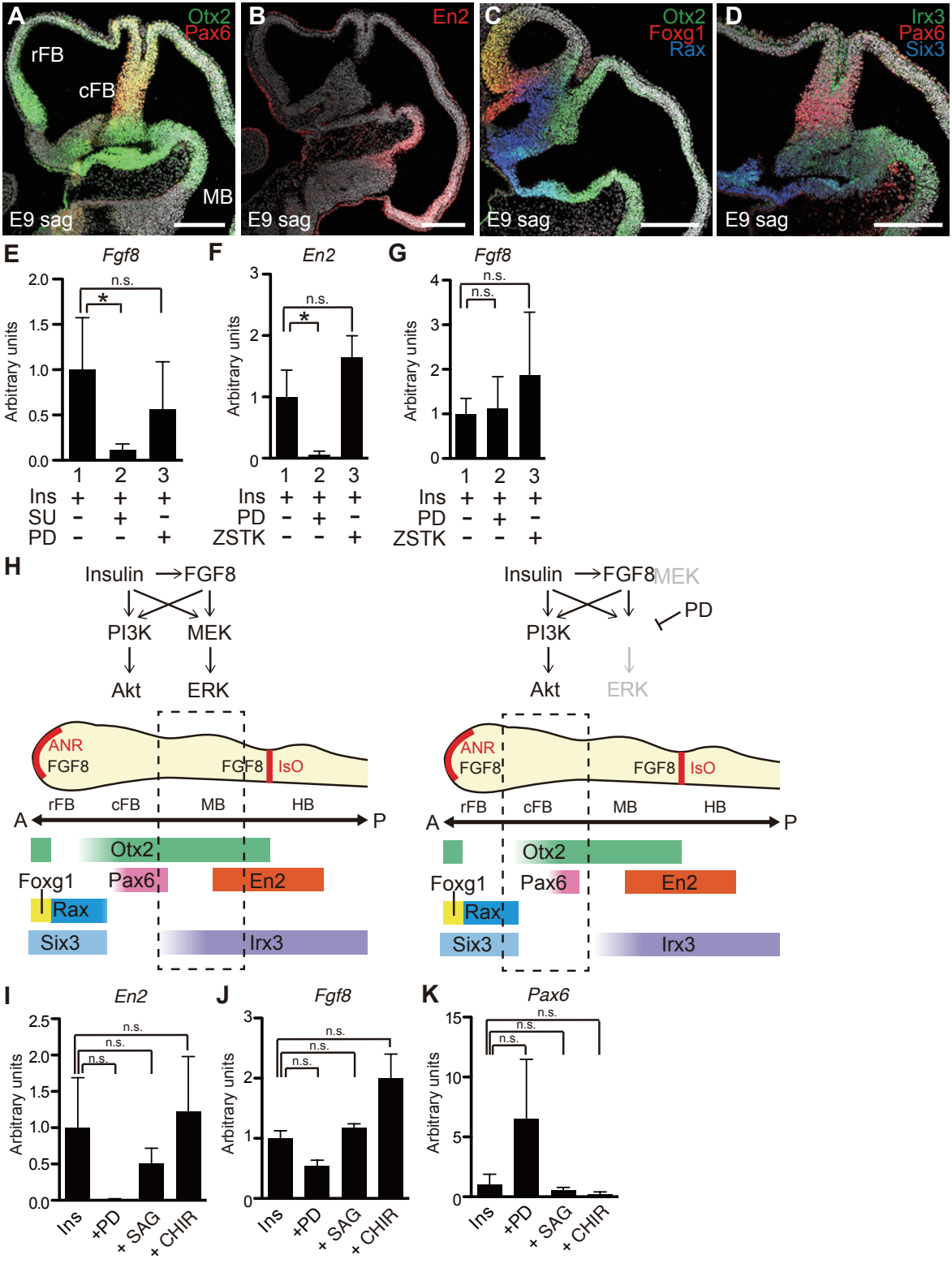
A
Otx2
Pax6
rFB
cFB
MB
E9 sag
B
En2
E9 sag
C
Otx2
Foxg1
Rax
E9 sag
D
Irx3
Pax6
Six3
E9 sag
E
Fgf8
Arbitrary units
n.s.
*
Ins
SU
PD
F
En2
Arbitrary units
n.s.
*
Ins
PD
ZSTK
G
Fgf8
Arbitrary units
n.s.
n.s.
Ins
PD
ZSTK
H
Insulin
FGF8
PI3K
MEK
Akt
ERK
ANR
FGF8
IsO
rFB
cFB
MB
HB
A
P
Otx2
Foxg1
Pax6
En2
Rax
Six3
Irx3
PD
I
En2
Arbitrary units
n.s.
Ins
+PD
+ SAG
+ CHIR
J
Fgf8
Arbitrary units
n.s.
K
Pax6
Arbitrary units
n.s.

Fig. S1. Effects of insulin and MEK inhibitor on anterior-posterior axis formation in SFEBq culture. (**A-D**) Expression of regional markers in the mouse E9 sagittal sections. Pax6 and Otx2 were co-expressed in caudal forebrain. (**E-G**) qPCR analysis of SFEBq-cultured mESC aggregates on day 7 for the expression of (E) Fgf8 (n = 40 aggregates from 5 independent experiments), (F) En2 and (G) Fgf8 (n = 96 aggregates in each from 6 independent experiments). Insulin (1 μg/ml) was added to the culture on day 0. FGF inhibitor (SU5402, 10 μM), MEK inhibitor (PD0325901, 1 μM) and PI3K inhibitor (ZSTK474, 250 nM) were added to the culture on day 4. Statistical differences were calculated between insulin-treated (lane 1) and additional treated mESCs (lane 2 and 3). (**H**) Schematic of caudal forebrain induction by the treatment with insulin and MEK inhibitor. (**I-K**) qPCR analysis of SFEBq-cultured mESC aggregates on day 7 for the expression of En2 (I), Fgf8 (J), and Pax6 (K) (n = 24 aggregates from 3 independent experiments). MEK inhibitor (PD0325901, 1 μM), Shh agonist (SAG, 10 nM) or GSK3β inhibitor (CHIR99021, 1 μM) were added to the culture on day 4. rFB, rostral forebrain; cFB, caudal forebrain; MB, midbrain; HB, hindbrain; ANR, anterior neural ridge; IsO, isthmic organizer. Scale bars: 200 μm in A-D. Each bars represents mean ± S.D. Nuclear counter staining (grey in A-D), DAPI.

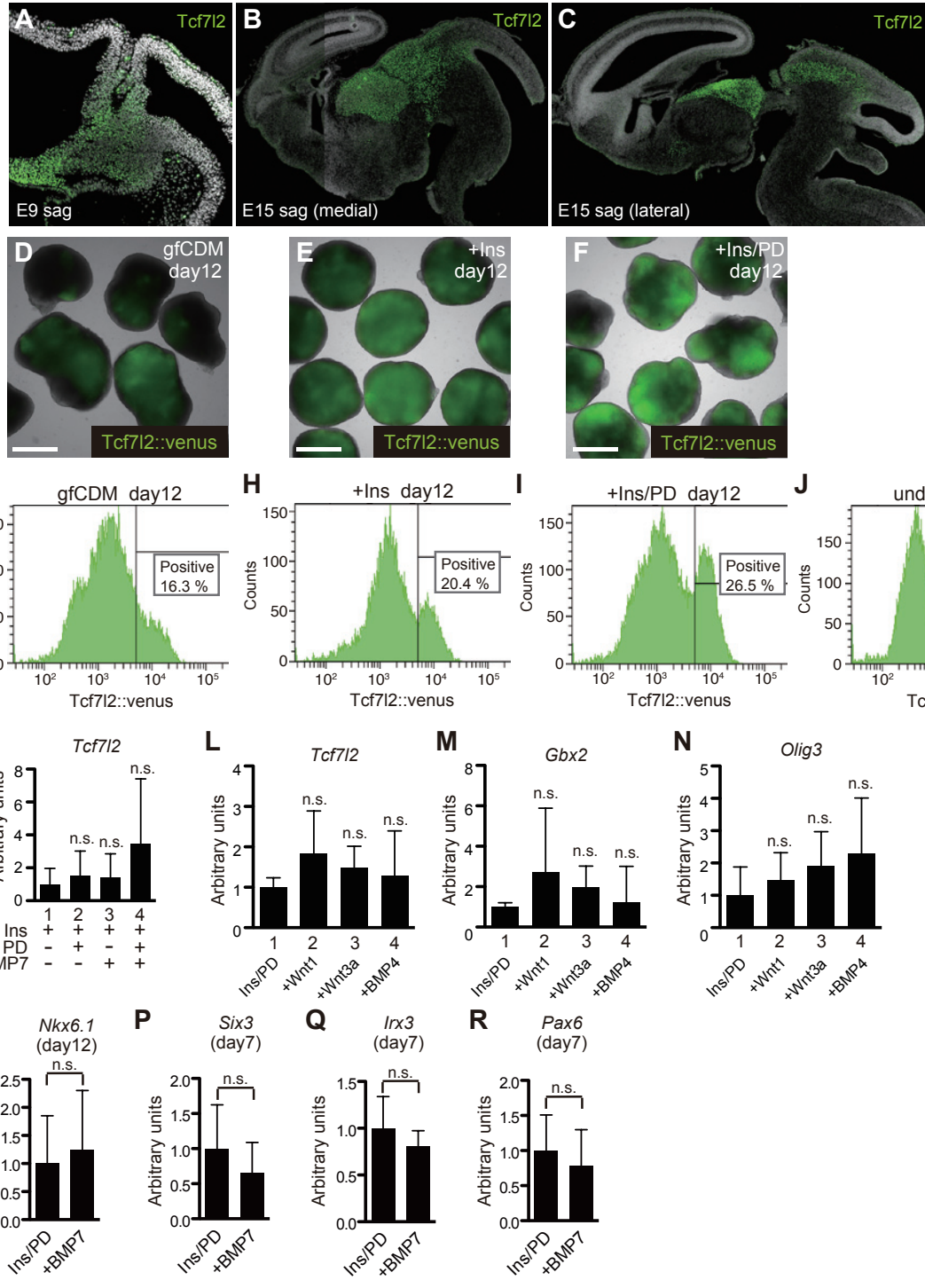

Fig. S2. BMP7 induces thalamic progenitors with little effects on anterior-posterior or dorso-ventral axes. (**A-C**) Expression of Tcf7l2 in the mouse E9 and E15 sagittal sections. (**D-F**) SFEBq-cultured mESC aggregates (Tcf7l2::venus) on day 12. (**G-J**) FACS analysis of Tcf7l2::venus fluorescence. (**K**) qPCR analysis of SFEBq-cultured mESC aggregates on day 12 for the expression of Tcf7l2 (n = 112 aggregates from 7 independent experiments). MEK inhibitor (1 μM) and/or BMP7 (30 ng/ml) were added to the culture on day 4. Statistical differences were calculated between insulin-treated (lane 1) and additional treated mESCs (lane 2-4). (**L-N**) qPCR analysis of SFEBq-cultured mESC aggregates on day 12 for the expression of Tcf7l2 (L), Gbx2 (M), and Olig3 (N) (n = 80 aggregates from 5 independent experiments). Wnt1 (50 ng/ml), Wnt3a (50 ng/ml), BMP4 (30 ng/ml) were added to the culture on day 4. Statistical differences were calculated between insulin/PD-treated (lane 1) and additional treated mESCs (lane 2-4). (**O**) qPCR analysis of SFEBq-cultured ESC aggregates on day 12 for the expression of Nkx6.1 (n = 80 aggregates from 5 independent experiments). BMP7 (30 ng/ml) was added to the culture on day 4. (**P-R**) qPCR analysis of SFEBq-cultured mESC aggregates on day 7 for the expression of Six3 (P), Irx3 (Q), or Pax6 (R) (n = 96 aggregates from 6 independent experiments). BMP7 (30 ng/ml) was added to the culture on day 4. Scale bars, 500 μm in D-F. Each bars represents mean ± S.D.

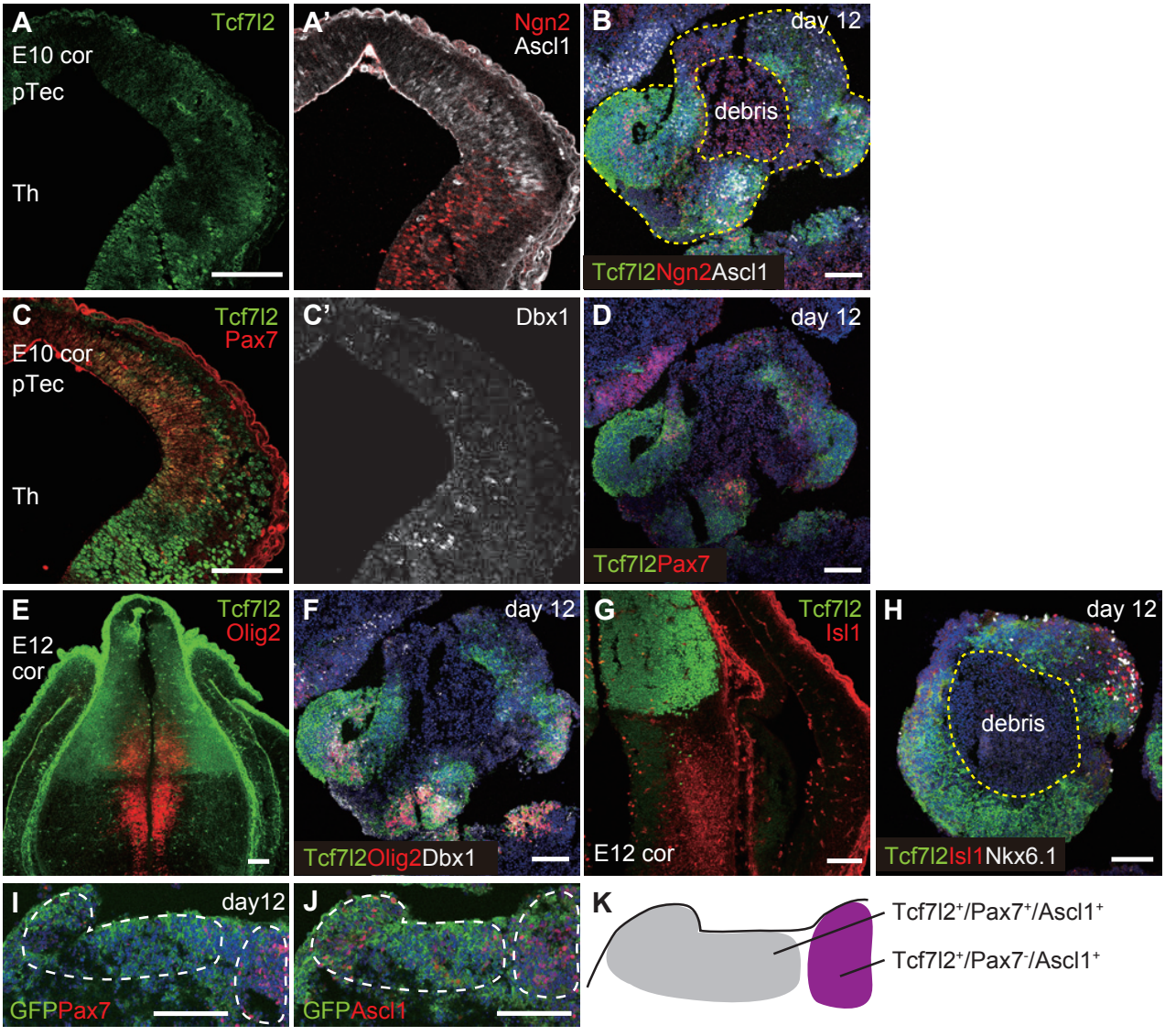

Fig. S3. Expression of specific markers for caudal forebrain in mESC-aggregates.

(**A,C,E,G**) Expression pattern of E12 caudal forebrain markers. (**B,D,F,H-J**) Cryosections of SFEBq-cultured mESC aggregate on day 12. (**K**) Schema for the expression pattern of thalamic markers in the mESC aggregate (I,J). Th, thalamus; pTec, pretectum. Yellow broken line demarcates the outline of the aggregate in (B, H). White broken line in (I, J) demarcates each structure in (K). Scale bars, 100 μm in A-J.

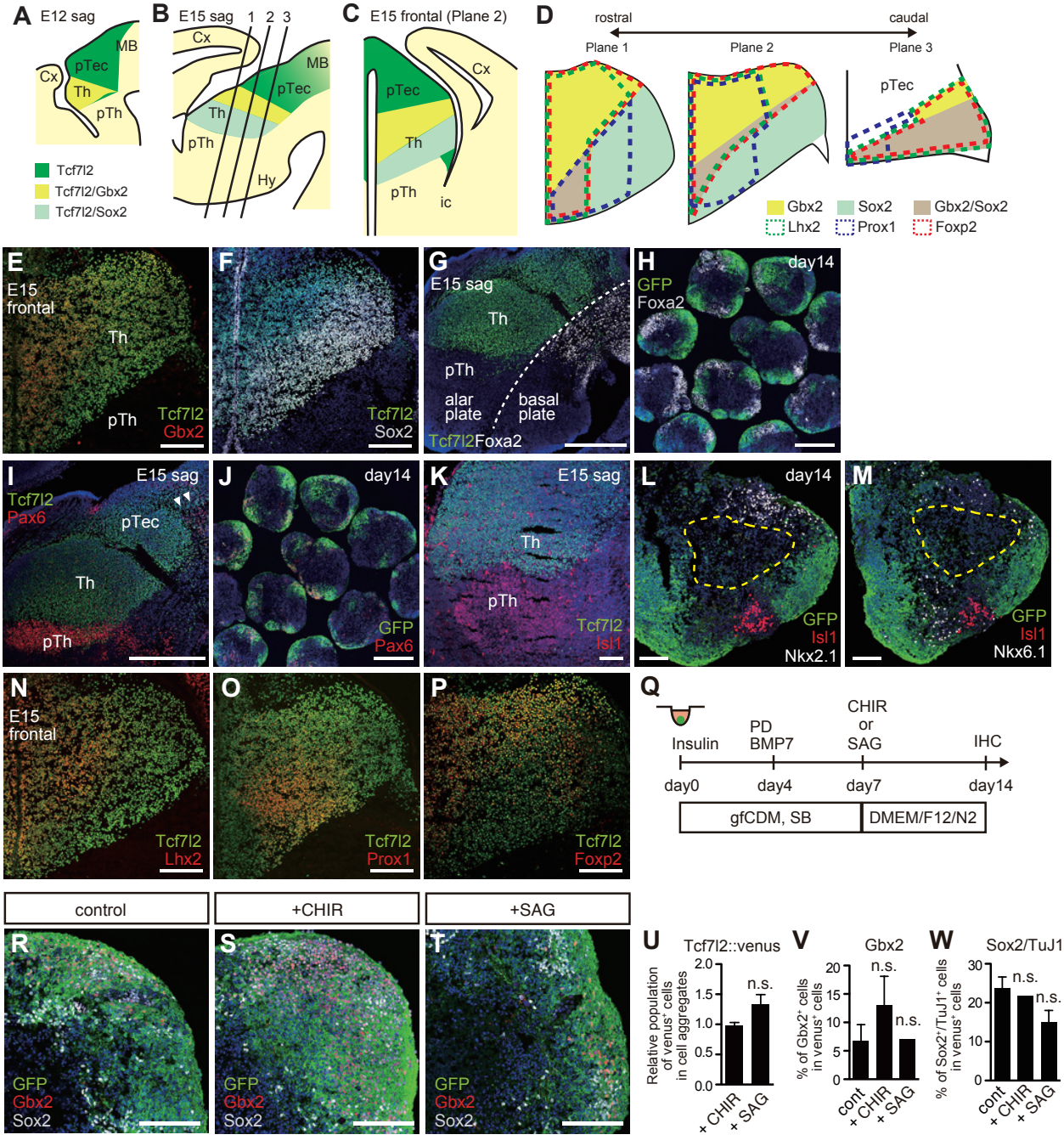

Fig. S4. Thalamic and non-thalamic populations in SFEBq-cultured mESC aggregates. (**A-D**) Schematic diagrams showing the expression patterns of thalamic markers in E12 and E15 mouse caudal forebrain. The lengthwise line represents the plane of frontal section. (**E,F**) Expression of thalamic neuronal markers in the E15 mouse frontal sections immunostained for Tcf7l2, Gbx2, and Sox2. (**G,H**) Expression of Tcf7l2 and basal plate marker Foxa2 in E15 mouse sagittal section (G) and mESC-aggregates on day14 (H). (**I**) Expression of Pax6 in prethalamus. Arrowheads indicate expression in pretectum. (**J**) Cryosection of aggregates on day 14, immunostained for GFP and Pax6. (**K**) E15 mouse sagittal section immunostained for Tcf7l2 and Isl1. (**L,M**) Cryosections of aggregate on day 14 immunostained with GFP, Isl1, Nkx2.1 and Nkx6.1. (**N-P**) Expression of thalamic neuronal markers in the E15 mouse frontal sections immunostained for Lhx2 (N), Prox1 (O), and Foxp2 (P) with Tcf7l2. (**Q**) Procedure for the differentiation of thalamic cells from ESC culture. CHIR99021 (1 μM) or SAG (10 nM) was added to the culture on day 7. (**R-T**) Sections of day 14 ESC aggregates cultured in SFEBq/IPB (R), SFEBq/IPB containing CHIR99021 (S), and SFEBq/IPB containing SAG (T). (**U**) Relative population of Tcf7l2::venus^{+} cells in DAPI^{+} cell aggregates on day 14 to those in the SFEBq/IPB culture (n = 48 aggregates from 3 independent experiments). (**V,W**) Percentage of cells expressing Gbx2^{+} (V) or Sox2^{+} (W) cells in Tcf7l2::venus-positive cells in aggregates on day 14 (n = 48 aggregates from 3 independent experiments). Cx, cortex; pTh, prethalamus; Th, thalamus; pTec, pretectum; MB, midbrain; Hy, hypothalamus; ic, internal capsule. Scale bars, 500 μm in G-J; 200 μm in E,F,N-P; 100 μm in K-M,R-T. Nuclear counter staining (blue), DAPI.

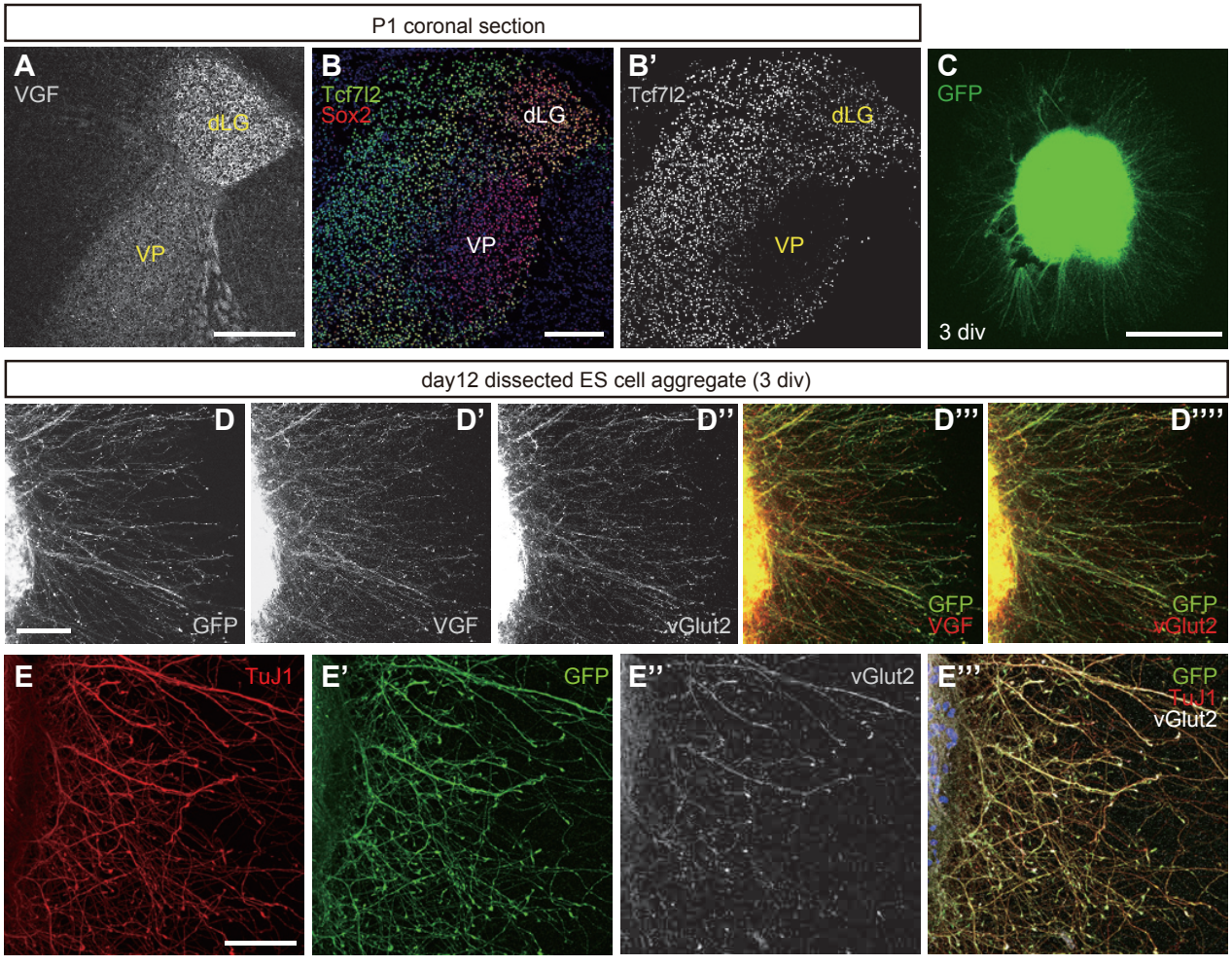

Fig. S5. Expression of Tcf7l2 in a part of thalamus diminishes by postnatal day 1. (**A-B'**) Expression pattern of VGF (A), Tcf7l2 and Sox2 (B) in P1 mouse coronal section. Of VGF^{+} sensory thalamic nuclei, ventroposterior nucleus decreased expression of Tcf7l2 by P1. (**C**) Tcf7l2::venus-positive potion dissected from ESC aggregate on day 12 at 3 days after collagen gel culture. The cells were immunostained with antibodies to GFP. (**D-D''''**) Neurites of dissected mESC-aggregate on day 15, immunostained with GFP, VGF, and vGlut2. (**E-E'''**) Neurites of dissected aggregate on day 15, immunostained with TuJ1, GFP and vGlut2. Scale bars, 200 μm in A,B; 500 μm in C; 100 μm in D,E. Nuclear counter staining (blue), DAPI.

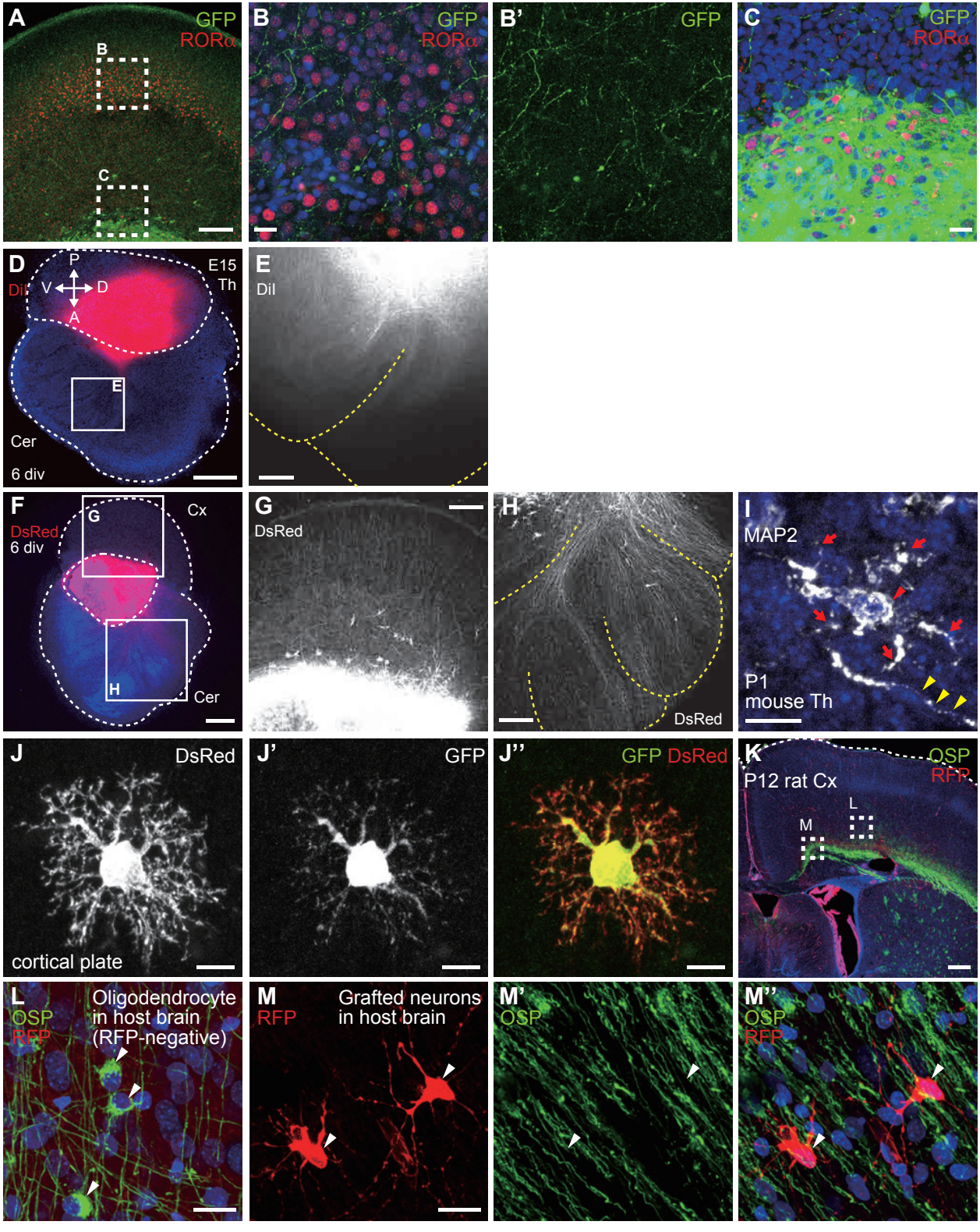
A
GFP
RORα
B
C
B
GFP
RORα
B'
GFP
C
GFP
RORα
D
P
V
D
A
Dil
E15
Th
E
Cer
6 div
E
Dil
F
G
Cx
DsRed
6 div
H
Cer
G
DsRed
H
DsRed
I
MAP2
P1
mouse Th
J
DsRed
cortical plate
J'
GFP
J''
GFP DsRed
K
OSP
RFP
P12 rat Cx
L
M
L
Oligodendrocyte
in host brain
(RFP-negative)
OSP
RFP
M
Grafted neurons
in host brain
RFP
M'
OSP
M''
OSP
RFP

Fig. S6. Ectopic projection or integration of thalamic neurons in co-culture or transplantation assay. (**A**) Co-culture of mESC-aggregate with postnatal day 1 (P1) rat cortical slice on culture day 6. (**B-C**) High-magnification views of insets in (A). (**D**) Co-culture of embryonic day 15 (E15) mouse thalamic explant and P1 rat cerebellar slice on culture day 6. DiI was injected in thalamic explant. (**E**) High-magnification view of the inset in (D). Note that thalamic neurons did not extend axons radially but preferentially along the white matter with fasciculation. (**F**) Triple culture of mESC aggregate, P1 rat cortical and cerebellar slices on culture day 6. (**G,H**) High-magnification view of the insets in (F). Yellow broken line in (H) demarcates the cerebellar explant. (**I**) Thalamic neurons in P1 mouse brain section. Red arrows and arrowhead indicate dendrites and soma, respectively. Yellow arrowheads indicate a neurite of another neuron. (**J**) A transplanted mESC-derived neuron in host rat cortex. (**K**) Host rat cortex at 1 week after transplantation. (**L-M"**) High-magnification view of the insets in (K). Cx, cortical slice; Cer, cerebellar slice. Scale bars, 200 μm in A,E,G,H; 20 μm in B,C,L,M; 10 μm in I,J; 500 μm in D,F,K. Nuclear counter staining (blue), DAPI.

Table S1. List of the genes and their primer sequences for qPCR analysis. GAPDH primers were used as an internal control for each specific gene amplification.

	Forward	Reverse
Six3	CCGGAAGAGTTGTCCATGTTC	CGACTCGTGTTTGTTGATGGC
Rax	TTCGAGAAGTCCCACTACCC	TTCATGGACGACACTTCCAG
Irx3	CAACGAGCACCGCAAGAA	TGGTGATGATGGCCAACATG
Fgf8	GTCCTGCCTAAAGTCACACAG	CTTCCAAAAGTATCGGTCTCCAC
En2	ATGGGACATTGGACACTTCTTC	CCCACAGACCAAATAGGAGCTA
Pax6	CAGCTTGGTGGTGTCTTTGT	GCAGAATTCGGGAAATGTCG
Otx2	CGTTCTGGAAGCTCTGTTTG	TTTTCAGTGCCACCTCTTCC
Tcf7l2	GGTGGCCGAATGCACATTGAAAGA	TTTGCCTGTTCT TCCCTGGACA
Gbx2	GCAAGGGAAAGACGAGTCAAA	GGCAAATTGTCATCTGAGCTGTA
Olig3	CAGGAGAGTCGTCTGAACTCG	GTTCGCGTCCGTTGATCTT
Nkx6.1	CTGCACAGTATGGCCGAGATG	CCGGGTTATGTGAGCCCAA
GAPDH	TGACCACAGTCCATGCCATC	GACGGACACATTGGGGGTAG